Neogene and Quaternary fossil remains of beaked whales (Cetacea, Odontoceti, Ziphiidae) from deep-sea deposits off Crozet and Kerguelen islands, Southern Ocean

Olivier Lambert, Christian De Muizon, Guy Duhamel, Johannes van Der Plicht

▶ **To cite this version:**

Olivier Lambert, Christian De Muizon, Guy Duhamel, Johannes van Der Plicht. Neogene and Quaternary fossil remains of beaked whales (Cetacea, Odontoceti, Ziphiidae) from deep-sea deposits off Crozet and Kerguelen islands, Southern Ocean. Geodiversitas, 2018, 40 (2), pp.135. 10.5252/geodiversitas2018v40a6 . hal-03888186

HAL Id: hal-03888186
https://hal.science/hal-03888186

Submitted on 7 Dec 2022

HAL is a multi-disciplinary open access archive for the deposit and dissemination of scientific research documents, whether they are published or not. The documents may come from teaching and research institutions in France or abroad, or from public or private research centers.

L'archive ouverte pluridisciplinaire **HAL**, est destinée au dépôt et à la diffusion de documents scientifiques de niveau recherche, publiés ou non, émanant des établissements d'enseignement et de recherche français ou étrangers, des laboratoires publics ou privés.

geodiversitas

2018 • 40 • 6

Neogene and Quaternary fossil remains of beaked whales (Cetacea, Odontoceti, Ziphiidae) from deep-sea deposits off Crozet and Kerguelen islands, Southern Ocean

Olivier LAMBERT, Christian de MUIZON,
Guy DUHAMEL & Johannes VAN DER PLICHT

art. 40 (6) — Published on 29 March 2018
www.geodiversitas.com

MUSÉUM
NATIONAL D'HISTOIRE NATURELLE
PUBLICATIONS SCIENTIFIQUES

Directeur de la publication : Bruno David,
Président du Muséum national d'Histoire naturelle

Rédacteur en chef / *Editor-in-chief* : Didier Merle

Assistants de rédaction / *Assistant editors* : Emmanuel Côtez (geodiv@mnhn.fr) ; Anne Mabille

Mise en page / *Page layout* : Emmanuel Côtez

Comité scientifique / *Scientific board* :
Christine Argot (MNHN, Paris)
Beatrix Azanza (Museo Nacional de Ciencias Naturales, Madrid)
Raymond L. Bernor (Howard University, Washington DC)
Alain Blieck (USTL, Villeneuve d'Ascq)
Henning Blom (Uppsala University)
Jean Broutin (UPMC, Paris)
Gaël Clément (MNHN, Paris)
Ted Daeschler (Academy of Natural Sciences, Philadelphie)
Bruno David (MNHN, Paris)
Gregory D. Edgecombe (The Natural History Museum, Londres)
Ursula Göhlich (Natural History Museum Vienna)
Jin Meng (American Museum of Natural History, New York)
Brigitte Meyer-Berthaud (CIRAD, Montpellier)
Zhu Min (Chinese Academy of Sciences, Pékin)
Isabelle Rouget (UPMC, Paris)
Sevket Sen (MNHN, Paris)
Stanislav Štamberg (Museum of Eastern Bohemia, Hradec Králové)
Paul Taylor (The Natural History Museum, Londres)

Couverture / *Cover* :
Réalisée à partir de la Figure 4 de cet article/*created from Figure 4 of this article.*

Geodiversitas est indexé dans / Geodiversitas *is indexed in:*
– Science Citation Index Expanded (SciSearch®)
– ISI Alerting Services®
– Current Contents® / Physical, Chemical, and Earth Sciences®
– Scopus®

Geodiversitas est distribué en version électronique par / Geodiversitas *is distributed electronically by:*
– BioOne® (http://www.bioone.org)

Les articles ainsi que les nouveautés nomenclaturales publiés dans *Geodiversitas* sont référencés par / *Articles and nomenclatural novelties published in* Geodiversitas *are referenced by:*
– ZooBank® (http://zoobank.org)

Geodiversitas est une revue en flux continu publiée par les Publications scientifiques du Muséum, Paris
Geodiversitas *is a fast track journal published by the Museum Science Press, Paris*

Les Publications scientifiques du Muséum publient aussi / *The Museum Science Press also publish:*
Adansonia, ***Zoosystema***, ***Anthropozoologica***, ***European Journal of Taxonomy***, ***Naturae***.

Diffusion – Publications scientifiques Muséum national d'Histoire naturelle
CP 41 – 57 rue Cuvier F-75231 Paris cedex 05 (France)
Tél. : 33 (0)1 40 79 48 05 / Fax : 33 (0)1 40 79 38 40
diff.pub@mnhn.fr / http://sciencepress.mnhn.fr

© Publications scientifiques du Muséum national d'Histoire naturelle, Paris, 2018
ISSN (imprimé / *print*) : 1280-9659/ ISSN (électronique / *electronic*) : 1638-9395

Neogene and Quaternary fossil remains of beaked whales (Cetacea, Odontoceti, Ziphiidae) from deep-sea deposits off Crozet and Kerguelen islands, Southern Ocean

Olivier LAMBERT
D.O. Terre et Histoire de la Vie, Institut royal des Sciences naturelles de Belgique, 29 rue Vautier, B-1000 Brussels (Belgium)
olivier.lambert@naturalsciences.be (corresponding author)

Christian de MUIZON
CR2P (CNRS, MNHN, UPMC, Sorbonne Université), Département Origines et Évolution, Muséum national d'Histoire naturelle, case postale 38, 57 rue Cuvier, F-75231 Paris cedex 05 (France)
muizon@mnhn.fr

Guy DUHAMEL
UMR BOREA (MNHN, UPMC, CNRS-7208, IRD-207, UCN, UA, Sorbonne Université), Département Adaptations du Vivant, Muséum national d'Histoire naturelle, case postale 26, 57 rue Cuvier, F-75231 Paris cedex 05 (France)
duhamel@mnhn.fr

Johannes VAN DER PLICHT
Center for Isotope Research, Faculty of Science and Engineering, Groningen University, Nijenborgh 6, 9747 AG Groningen (the Netherlands)
j.van.der.plicht@rug.nl

Submitted on 7 September 2017 | accepted on 24 November 2017 | published on 29 March 2018

urn:lsid:zoobank.org:pub:06EB756D-EE16-4B28-A09C-EA983B758397

Lambert O., Muizon C. de, Duhamel G. & van der Plicht J. 2018. — Neogene and Quaternary fossil remains of beaked whales (Cetacea, Odontoceti, Ziphiidae) from deep-sea deposits off Crozet and Kerguelen islands, Southern Ocean. *Geodiversitas* 40 (6): 135-160. https://doi.org/10.5252/geodiversitas2018v40a6. http://geodiversitas.com/40/6

ABSTRACT
Although a high number of extant beaked whale species (Cetacea, Odontoceti, Ziphiidae) live in the Southern Ocean and neighbouring areas, only little is known about the past occupation of the region by these highly specialized, deep diving and echolocating cetaceans. Recently, longline fishing activities along the seafloor at depths of 500-2000 m off the sub-antarctic Crozet and Kerguelen islands, Indian sector of Southern Ocean, resulted in the accessory "capture" of tens of ziphiid fossil cranial remains. Our description and comparison of the best-preserved and most diagnostic crania from this sample lead to the identification of more than eight species in at least seven genera: the hyperoodontines *Africanacetus ceratopsis*, *Khoikhoicetus kergueleni* n. sp., Hyperoodontinae indet. aff. *Africanacetus*, and *Mesoplodon* sp. aff. *Mesoplodon layardii*, the ziphiines *Izikoziphius rossi* and *Ziphius* sp., and the ziphiids indet. *Nenga* sp. aff. *Nenga meganasalis* and *Xhosacetus hendeysi*.
Unsurprisingly, with at least four species in common (*A. ceratopsis*, *Izikoziphius rossi*, *X. hendeysi*, and *Ziphius* sp.), the assemblage displays high similarities with assemblages described from deep-sea deposits off South Africa, providing thus new data on the palaeogeographic distribution of several extinct species and indicating a roughly similar geochronological age for at least a part of the as-

KEY WORDS
Ziphiidae,
beaked whale,
Kerguelen Islands,
Crozet Islands,
Miocene,
Quaternary,
Southern Ocean,
new species.

semblages. The limited amount of data available points to a pre-Pliocene age for a large part of the Crozet-Kerguelen assemblage, suggesting a relatively early, Miocene colonization of the Southern Ocean by crown ziphiids. Contrastingly, ^{14}C radiometric dating of two specimens of *Mesoplodon* sp. aff. *Mesoplodon layardii* yielded latest Pleistocene-earliest Holocene ages. These results reveal the presence either of an extinct species of *Mesoplodon* in the Southern Ocean only a few thousands years ago, or of an up-to-now unidentified extant species closely related to the strap-toothed whale *M. layardii*.

RÉSUMÉ

Restes fossiles néogènes et quaternaires de baleines à bec (Cetacea, Odontoceti, Ziphiidae) de dépôts profonds au large des îles Crozet et Kerguelen, océan Austral.

Bien qu'un grand nombre d'espèces de baleines à bec (Cetacea, Odontoceti, Ziphiidae) habitent de nos jours l'océan Austral et les zones avoisinantes, l'occupation passée de cette région par ces cétacés à sonar hautement spécialisés, se nourrissant à grandes profondeurs, reste très mal connue. Récemment, des activités de pêche à la palangre menées sur le fond de l'océan à des profondeurs de 500 à 2000 mètres au large des îles sub-antarctiques de Crozet et Kerguelen, dans le secteur indien de l'océan Austral, ont permis la « capture » accessoire de dizaines de restes crâniens fossiles de ziphiidés. La description et la comparaison des crânes les mieux préservés et les plus diagnostiques de cette collection a permis l'identification de plus de huit espèces dans au moins sept genres : les hyperoodontinés *Africanacetus ceratopsis*, *Khoikhoicetus kergueleni* n. sp., Hyperoodontinae indet. aff. *Africanacetus*, et *Mesoplodon* sp. aff. *Mesoplodon layardii*, les ziphiinés *Izikoziphius rossi* et *Ziphius* sp., et les ziphiidés indet. *Nenga* sp. aff. *Nenga meganasalis* et *Xhosacetus hendeysi*.

Sans surprise, avec au moins quatre espèces en commun (*A. ceratopsis*, *Izikoziphius rossi*, *X. hendeysi*, et *Ziphius* sp.), cet assemblage montre les plus grandes similitudes avec les assemblages décrits des dépôts océaniques profonds au large de l'Afrique du Sud. Ces similitudes fournissent de nouvelles données sur la distribution paléogéographique de plusieurs espèces éteintes et indiquent des âges géochronologiques similaires pour au moins une partie de ces assemblages. La quantité limitée de données disponibles indique un âge pré-Pliocène pour une bonne partie de l'assemblage de Crozet-Kerguelen, ce qui suggère une colonisation relativement précoce de l'océan Austral par des ziphiidés du groupe-couronne. D'un autre côté, la datation radiométrique au ^{14}C de deux spécimens de *Mesoplodon* sp. aff. *Mesoplodon layardii* a fourni des âges allant du Pléistocène terminal au tout début de l'Holocène. Ces résultats indiquent soit la présence d'une espèce éteinte de *Mesoplodon* dans l'océan Austral il y a seulement quelques milliers d'années, soit la présence d'une espèce moderne, non encore identifiée et proche parente de la baleine à bec de Layard *Mesoplodon layardii*.

MOTS CLÉS
Ziphiidae,
baleines à bec,
Îles Kerguelen,
Îles Crozet,
Miocène,
quaternaire,
océan austral,
espèce nouvelle.

INTRODUCTION

Beaked whales (Cetacea, Odontoceti, Ziphiidae) are a diversified family of echolocating toothed whales. The ecologically highly specialized extant species feed at great depths and via suction on cephalopods and, to a lesser extent, fish (Heyning & Mead 1996; McLeod *et al.* 2003; Tyack *et al.* 2006; Schorr *et al.* 2014). Among those, at least 10 species in 5 genera live in the Southern Ocean and neighbouring areas, where they constitute key components of the deep benthopelagic to benthic communities (McLeod *et al.* 2006). Although the fossil record of ziphiids is continuously improving (e.g. Buono & Cozzuol 2013; Bianucci *et al.* 2016; Ramassamy 2016), inland localities were up to now of little use to trace the past occupation of the oceanic regions surrounding the Antarctic. However, many new fossil taxa were recently described from deep-sea deposits, including localities from off South Africa and the southernmost part of the Kerguelen Plateau, Southern Ocean (Bianucci *et al.* 2007, 2008; Gol'din & Vishnyakova 2012). Although the description of the South African fauna(s) provided a first glimpse of the past ziphiid biodiversity in a region at the northern margin of the Southern Ocean, it was up to now not possible to determine the effective distribution in this oceanic area for most of the taxa – an exception being the hyperoodontine genus *Africanacetus* Bianucci, Lambert & Post, 2007, found both along South Africa and close to the Antarctic continent (Bianucci *et al.* 2007; Gol'din & Vishnyakova 2012).

Commercial bottom longline fishing activities at depths of 500 to 2000 meters off the sub-Antarctic Crozet and Kerguelen islands, Indian sector of Southern Ocean (see Duhamel & Williams 2011), occasionally result in the accessory "capture" of fossil cranial elements attributed to the family Ziphiidae. Thanks to regular contacts between fishermen and scientists working in the area, first fossil discoveries reporting conduct to establish a long-term protocol to collect any specimens and transport them at the Muséum national d'Histoire naturelle (Paris, France). It resulted in the gathering of a large sample. The study of this sample eventually lead to the identification, description, and comparison of more than eight species in at least seven genera.

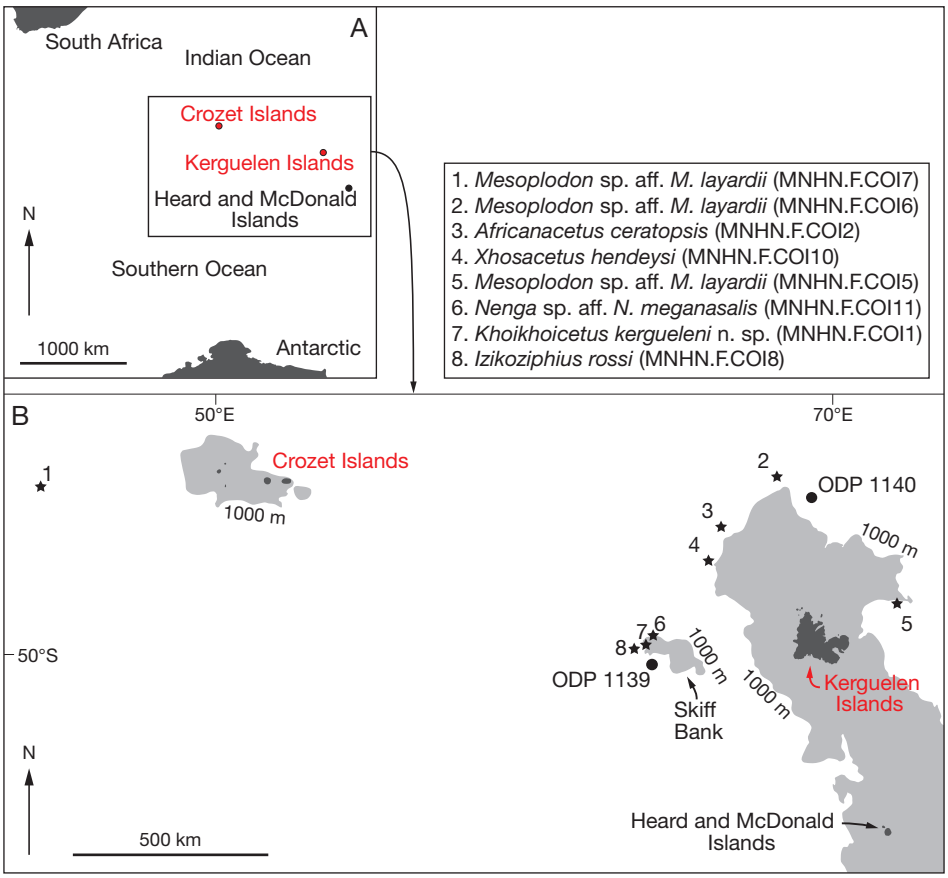

FIG. 1. — Locality maps: **A**, schematic map providing the position of Crozet and Kerguelen islands in the Southern Ocean; **B**, schematic map of the Crozet and Kerguelen islands area, including the main localities where fossil ziphiid specimens (★) described in this work were found via longline fishing, as well as two ODP sites (●). **Light grey** shading for areas with a water depth lower than 1000 m; **dark grey** shading for islands and continents.

When studying fossil remains from deep-sea deposits, the lack of a well-constrained geological and, more specifically, chronostratigraphic context is often a major weakness (Bianucci *et al.* 2007, 2013, but see Ichishima *et al.* 2017; Nozaki *et al.* 2017). Whereas the discovery of a few Quaternary cranial remains off Crozet and Kerguelen islands allowed ^{14}C datings for two specimens, the combination of data from local Oceanic Drilling Program sections with ziphiid faunal comparisons provides clues for a pre-Pliocene origin for another part of the sample.

MATERIAL AND METHODS

INSTITUTIONAL ABBREVIATIONS

MNHN	Muséum national d'Histoire naturelle, Paris;
NMR	Natuurhistorisch Museum Rotterdam, Rotterdam;
PEM	Port Elizabeth Museum, Port Elizabeth;
SAM	Iziko South African Museum, Cape Town.

SPECIMENS

Most of the fossil ziphiid remains described here were collected in the past seven years with tens of other, more fragmentary cetacean specimens (mostly including rostral fragments, but also one tympanic bulla attributed to the delphinid genus *Orcinus*) during commercial longline fishing activities targeting the deep water Patagonian toothfish *Dissostichus eleginoides* at depths of 500 to 2000 meters off the sub-Antarctic Crozet and Kerguelen islands, Indian sector of the Southern Ocean (Duhamel & Williams 2011) (Fig. 1). Two specimens (MNHN.F.COI12 and COI13) were discovered several tens of years ago and lack any information about the details of collection. All the specimens are now curated at the MNHN.

RADIOMETRIC DATING

Two partial ziphiid crania, MNHN.F.COI5 and COI6, were sampled for radiocarbon (^{14}C) dating. For each specimen, a small fragment of bone was removed. The datable fraction of bone being collagen, the latter was extracted following an improved version of the protocol originally developed by Longin (Longin 1971; Mook & Streurman 1983). The quality of the bone collagen was assessed by the atomic C/N ratio, as well as its C and N content. These numbers should be in specified ranges (DeNiro 1985; Ambrose 1990): the atomic C/N ratio should be *c.* 2.9-3.6, the carbon content of the collagen (C%) *c.* 30-45%, and the nitrogen content (N%) *c.* 11-16%. Values outside this range may indicate diagenetic alteration causing

changes to the organic composition of the sample. The collagen was combusted into CO_2 or N_2 gas by an Elemental Analyzer, coupled to an Isotope Ratio Mass Spectrometer. This setup provides the stable isotopes ratios $\delta^{13}C$ and $\delta^{15}N$. Part of the CO_2 was cryogenically trapped for ^{14}C analysis. This CO_2 was reduced to graphite by the Bosch reaction: $CO_2 + 2H_2 \rightarrow C + 2H_2O$, using Fe as a catalyst at a temperature of 600°C (Aerts *et al.* 2001). The graphite was pressed into a sample holder, which was placed in the ion source of the Accelerator Mass Spectrometer (AMS). The Groningen AMS is a tandetron, based on a 2.5 MV particle accelerator (van der Plicht *et al.* 2000).

The results are reported in conventional radiocarbon years (BP), which implies measuring relative to the Oxalic Acid standard, correction for isotopic fractionation using the stable isotope ratio $^{13}C/^{12}C$ to $\delta^{13}C = -25‰$, and using a half-life value of 5568 years (Mook & van der Plicht 1999). Because of fluctuations in the natural ^{14}C content, the ^{14}C ages have to be calibrated into calendar ages. This is done with the calibration curve IntCal13 (Reimer *et al.* 2013). The calibrated ages are reported in calBP, which is calender years relative to AD 1950. Organisms living in aquatic reservoirs show apparent ages known as reservoir effects, caused by different ^{14}C concentrations in contemporaneous terrestrial and aquatic reservoirs. The size of the reservoir effect is 400 years for marine organisms. This number has to be subtracted from the ^{14}C date before calibration (Reimer *et al.* 2013).

The stable isotopic content of the samples is expressed in delta (δ) values, which are defined as the deviation (expressed in per mil) of the rare to abundant isotope ratio from that of a reference material:

$$^{13}\delta = \frac{(^{13}C/^{12}C)_{sample}}{(^{13}C/^{12}C)_{reference}} - 1 \ (\times 1000‰)$$

and

$$^{15}\delta = \frac{(^{15}N/^{14}N)_{sample}}{(^{15}N/^{14}N)_{reference}} - 1 \ (\times 1000‰)$$

For carbon, the reference material is belemnite carbonate (V-PDB); for nitrogen, the reference is ambient air (Mook 2006). The analytical error is 0.1‰ and 0.2‰ for $\delta^{13}C$ and $\delta^{15}N$, respectively.

GEOLOGICAL CONTEXT

The geology of sedimentary deposits from the deep seafloor off Kerguelen and Crozet islands is relatively poorly known; local investigations mostly focused on the hot spot-related, long-term volcanic activity and only a limited number of deep-sea drillings were performed in the area (e.g. Cottin *et al.* 2011). Among those, two Oceanic Drilling Program (ODP) sites of Leg 183 (1139 and 1140) from the Kerguelen plateau are close enough to fossil ziphiid finds to deserve some comments (Reusch 2002; McCartney *et al.* 2003; Bénard *et al.* 2010; Fig. 1). At a depth of 1450 m on the southwest flank of Skiff Bank, 350 km SWW to Kerguelen Islands, site 1139 is located in a region where at least nine cranial remains of ziphiids were found (see below for the most significant specimens). Site 1140 is similarly close to several ziphiid finds, 270 km north to Kerguelen Islands, but somewhat deeper (2394 m). Following the Eocene formation of basalts and other igneous rocks and the deposition of Oligocene sands, grainstones, dolomitic chalk, and foraminifer-bearing oozes, Miocene sediments include more homogenous deposits of foraminifer-bearing shales at site 1139 and nannofossil- and foraminifer-bearing pelagic oozes at site 1140. Up to several meters thick Pleistocene to Holocene deposits include diatom oozes, with organic debris at site 1139 (Bénard *et al.* 2010). Interestingly, an important hiatus is recorded in both sites, extending from late middle Miocene to late Pliocene, as indicated by diatoms and silicoflagellates (Reusch 2002; Arney *et al.* 2003; McCartney *et al.* 2003; Bénard *et al.* 2010).

SYSTEMATIC PALAEONTOLOGY

Order CETACEA Brisson, 1762
Clade NEOCETI Fordyce & Muizon, 2001
Suborder ODONTOCETI Flower, 1867
Family ZIPHIIDAE Gray, 1850
Subfamily HYPEROODONTINAE Gray, 1866
sensu Bianucci *et al.* (2016)

Genus *Khoikhoicetus* Bianucci, Lambert & Post, 2007

TYPE SPECIES. — *Khoikhoicetus agulhasis* Bianucci, Lambert & Post, 2007 by original designation.

OTHER SPECIES INCLUDED. — *Khoikhoicetus kergueleni* n. sp.

Khoikhoicetus kergueleni n. sp.

urn:lsid:zoobank.org:act:2543332B-3F91-4890-8A85-93EB8A3B11E0

HOLOTYPE. — MNHN.F.COI1, partial cranium including the complete rostrum the anterior part of the cranium with a large part of the face, premaxillary sac fossae, the bony nares, part of both supraorbital regions, and the vertex (Fig. 2).

TYPE LOCALITY. — The holotype has been fished on Skiff Bank, 370 km SWW to Kerguelen Islands at a depth of 885 m; geographic coordinates 49°49'17.4"S, 63°37'33.6"E (Fig. 1).

REFERRED SPECIMEN AND LOCALITY. — Partial cranium MNHN.F.COI13 including rostrum, premaxillary sac fossae, part of both supraorbital regions, and vertex (Fig. 3); off Kerguelen Islands, no indication about the precise locality is available.

ETYMOLOGY. — In memory of Yves Joseph de Kerguelen de Trémarec (1734-1797), rear admiral of the French Royal Navy, who took possession of the "îles de la Désolation" (later designated by James Cook "Kerguelen Archipelago") for the crown of France in 1772.

DIAGNOSIS. — *Khoikhoicetus kergueleni* n. sp. differs from *Khoikhoicetus agulhasis* in the following features: larger size; outline of the rostrum in dorsal view distinctly triangular with straight lateral edges; dorsal infraorbital foramen notably distant from the maxilla-premaxilla suture (from 10 to 20 mm); premaxillary sac fossae signifi-

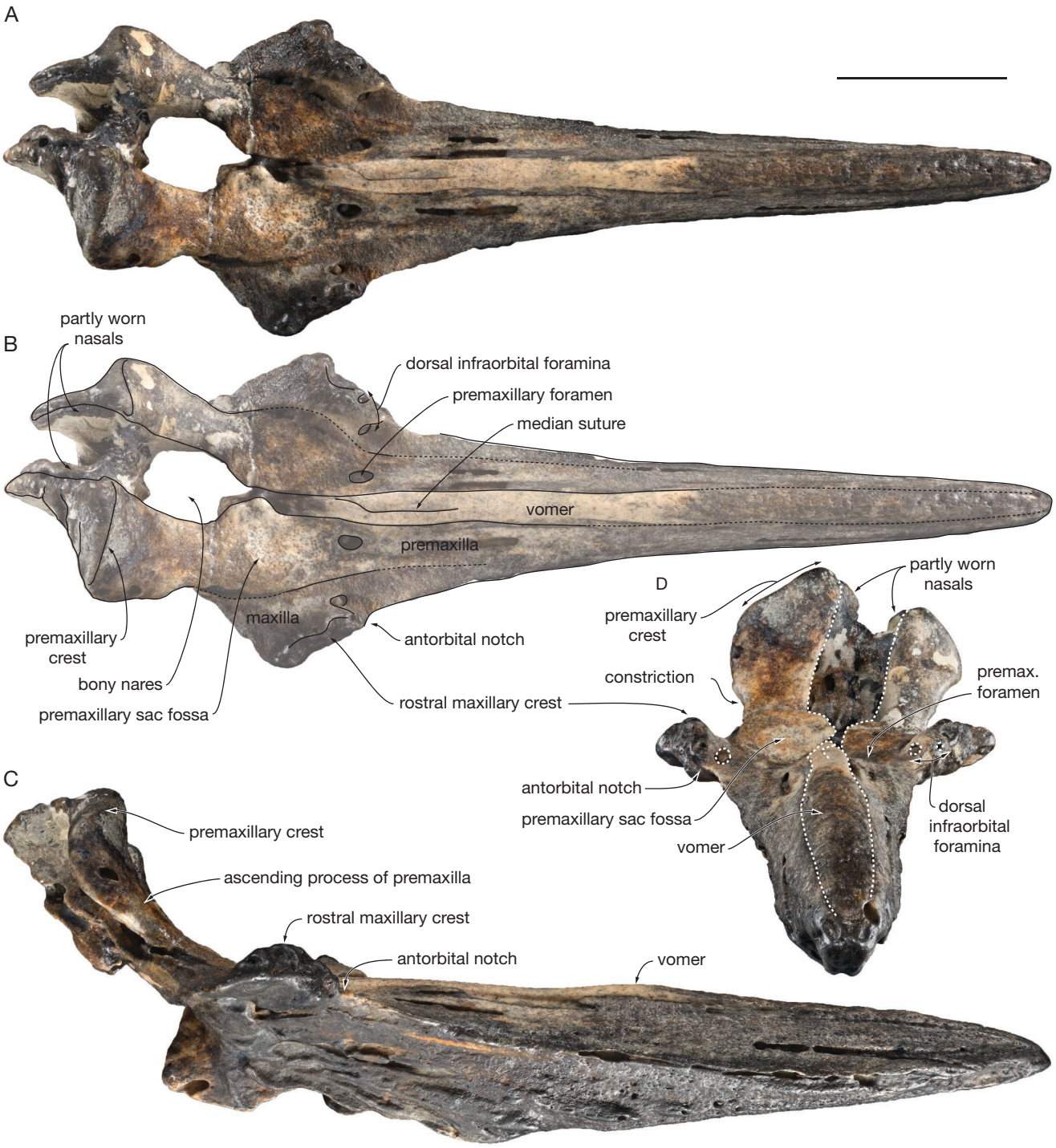

Fig. 2. — Partial cranium of *Khoikhoicetus kergueleni* n. sp. (MNHN.F.COI1): **A**, dorsal view; **B**, same view with interpretive line drawing; **C**, right lateral view; **D**, anterodorsal view. Scale bar: 100 mm.

cantly proportionally narrower; bony nares relatively narrower and roughly oval-shaped; premaxillary crests anteroposteriorly thicker and wider (in anterior view) than the premaxillary sac fossae; and premaxillary crests located posterior to the premaxillary sac fossae (in lateral view), and not overhanging them.

Brief description and comparison

Completely preserved, the rostrum of both specimens is higher than wide for most of its length. The lateral edges of the rostrum are roughly straight in dorsal view and regularly diverge posteriorly until the antorbital notches. The rostrum of MNHN.F.COI13 is more massive and widens posteriorly more abruptly than on COI1. The mesorostral groove is completely filled by the vomer, which is dorsally higher than the adjoining premaxilla for its whole length. This condition is more accentuated in COI1, in which the vomer forms a small dome in the mid-length region of the rostrum. A median suture marks the posterior portion

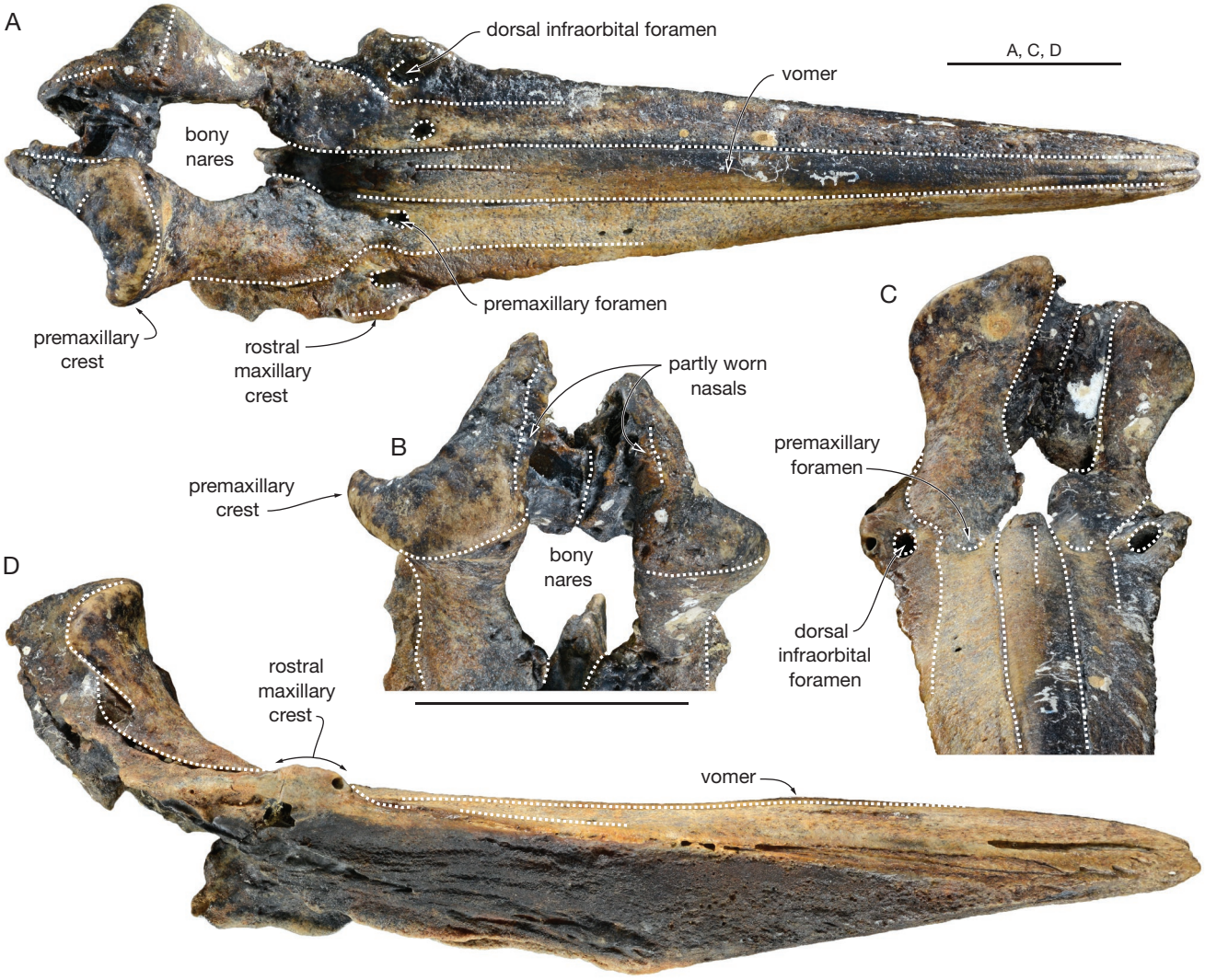

Fig. 3. — Partial cranium of *Khoikhoicetus kergueleni* n. sp. (MNHN.F.COI13): **A**, dorsal view; **B**, detail of the vertex in dorsal view; **C**, anterodorsal view; **D**, right lateral view. Scale bars: 100 mm.

Table 1. — Measurements (in mm) on the partial crania of *Khoikhoicetus kergueleni* n. sp. MNHN.F.COI1 (holotype), MNHN.F.COI13, and *Khoikhoicetus agulhasis* Bianucci, Lambert & Post, 2007 SAM PQ 2678 (holotype) (from Bianucci *et al.* 2007). Abbreviations: **e**, estimate; **+**, not complete; **–**, no data.

	***Khoikhoicetus kergueleni* n. sp.**		***Khoikhoicetus agulhasis***
	MNHN.F.COI1 (holotype)	**MNHN.F.COI13**	**SAM PQ 2678 (holotype)**
Rostrum length	415	e455	–
Height of rostrum at mid-length	73	83	–
Width of rostrum at mid-length	54	74	–
Maximum opening of mesorostral groove	25	32	24
Width of rostrum at base	e125	e134	120
Width of premaxillae at rostrum base	66	84	49
Width of premaxillary sac fossae	108	133e	106
Width of right premaxillary sac fossa	59	62	50
Width of left premaxillary sac fossa	47	e54	48
Width of bony nares	47	55	43
Minimum width of right ascending process of premaxilla	38	45	25
Width of premaxillary crests	142	166	+100
Width of right premaxillary crest	62	78	+33
Width of left premaxillary crest	46	52	30
Minimum distance between premaxillary crests	40	43	34
Maximum width of nasals	48	53	45
Minimum posterior distance between maxillae	e34	34	38

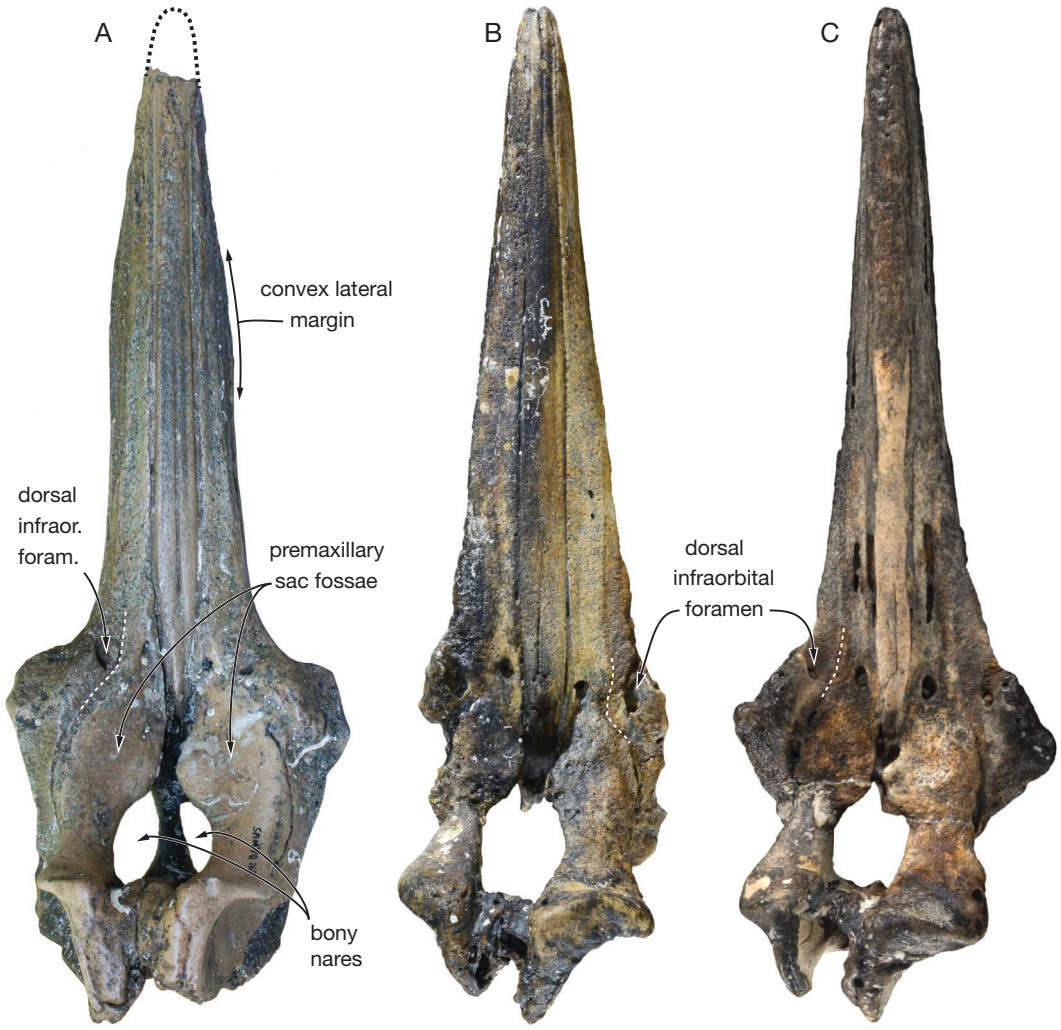

FIG. 4. — Comparison of the cranium of *Khoikhoicetus agulhasis* Bianucci, Lambert & Post, 2007 and *Khoikhoicetus kergueleni* n. sp.: **A**, *Khoikhoicetus agulhasis* SAM PQ 2678 (holotype, photo G. Bianucci); **B**, *Khoikhoicetus kergueleni* n. sp. (MNHN.F.COI1, holotype); **C**, *K. kergueleni* n. sp. (MNHN.F.COI13), in dorsal view. **Dotted line** for the reconstructed apex of the rostrum of SAM PQ 2678. All crania scaled to the same distance from apex of rostrum to anterior margin of bony nares.

TABLE 2. — Comparison of the relative width of the bony nares in the two specimens of *Khoikhoicetus kergueleni* n. sp. (MNHN.F.COI1 and COI13) and the holotype of *Khoikhoicetus agulhasis* Bianucci, Lambert & Post, 2007 (SAM PQ 2678). Measurements in mm. Abbreviations: **Pona**, length of skull from apex of rostrum to posteriormost edge of nasals; **Wdiof**, width between the main dorsal infraorbital foramina; **Wn**, width of the bony nares; **Wpf**, width between the premaxillary foramina. Pona for SAM PQ 2678 has been estimated as explained in the text. Measurements of Wpf, Wdiof, and Pona for SAM PQ 2678 have been calculated form Bianucci *et al.* (2008: fig. 13A) and therefore represent an approximation.

	Wn	Wpf	Wdiof	Pona	Wn/Wpf	Wn/Wdiof	Wn/Pona
SAM PQ 2678	43	23.8	56	396e	1.8	0.77	0.108
MNHN.F.COI1	47	40	102.5	587	1.17	0.49	0.0800
MNHN.F.COI13	55	52	121	660	1.05	0.45	0.083

of the vomer. The rostral maxillary crest forms an elevated, but relatively short dome in the antorbital region. Located medial to the crest, the medium-sized main dorsal infraorbital foramen is opening anteriorly to anteromedially, roughly at the same anteroposterior level as the premaxillary foramen, but higher dorsally than the latter (best seen in anterior view of MNHN.F.COI1). In COI13 the main dorsal infraorbital foramen is two to three times larger than on the other specimen and opens slightly posterior to the premaxillary foramen. The premaxillary foramen is large, especially on COI13, in which it opens posteriorly and extends as a wide and deep groove running toward the anteromedial area of the premaxillary sac fossa. It is slightly posterior to the antorbital notch on both specimens. Anteriorly defining the bony nares, the medialmost angle of the right premaxillary sac fossa projects medially. A similar medial projection is observed on the left side, but it is less protruding and more rounded. The lateral margin of the ascending process of the premaxilla (*sensu* Bianucci *et al.* 2007) displays a marked constriction in anterior view. The medial margins of the right and left ascending processes converge slightly dorsally,

TABLE 3. — Comparison of the relative width of the premaxillary sacs fossae in the two specimens of *Khoikhoicetus kergueleni* n. sp. (MNHN.F.COI1 and COI13) and the holotype of *Khoikhoicetus agulhasis* Bianucci, Lambert & Post, 2007 (SAM PQ 2678). Measurements in mm. Abbreviations: **Pona**, length of skull from apex of rostrum to posteriormost edge of nasals; **Wdiof**, width between the dorsal infraorbital foramina; **Wpf**, width between the premaxillary foramina; **Wpsf**, width of the premaxillary sac fossae. Pona for SAM PQ 2678 has been estimated as explained above. Measurements of Wpf, Wdiof, and Pona have been calculated form Bianucci *et al.* (2008: fig. 13A) and therefore represent an approximation.

	Wpf	Wpsf	Wdiof	Pona	Wpf/Wpsf	Wdiof/Wpsf	Wpsf/Pona
SAM PQ 2678	23.8	106	56	396e	0.22	0.53	0.267
MNHN.F.COI1	40	108	102.5	587	0.37	0.95	0.184
MNHN.F.COI13	52	133e	121	660	0.39	0.91	0.201

TABLE 4. — Comparison of the individual variation of the width of the premaxillary sac fossae and of the width of the bony nares in two samples of extant ziphiids (*Mesoplodon densirostris* (Blainville, 1817) and *M. layardii* (Gray, 1865)) and in our fossil sample of *Khoikhoicetus* Bianucci, Lambert & Post, 2007. Abbreviations: **min**, minimum value measured for the extant sample in Ross (1984) or in the extinct *Khoikhoicetus*; **max**, maximum value measured for the extant sample in Ross (1984) or in the extinct *Khoikhoicetus*; **Wn**, width of the external bony nares; **Wpsf**, width of the premaxillary sac fossae.

	min	max	max–min	% of min
Mesoplodon densirostris (Wpsf)	14.2	15.1	0.9	6.3%
Mesoplodon layardii (Wpsf)	10.6	12.5	1.9	17%
Khoikhoicetus (Wpsf)	0.184	0.267	0.083	45%
Mesoplodon densirostris (Wn)	5.5	6.6	1.1	20%
Mesoplodon layardii (Wn)	5.2	6.8	1.6	30%
Khoikhoicetus (Wn)	0.08	0.108	0.028	35%

and the posterodorsal part of the anterior surface is subvertical, but does not overhang the more ventral part of the ascending process. The markedly asymmetric premaxillary crests are directed slightly posterolaterally, and the dorsal margin of each crest slopes abruptly ventrolaterally in anterior view. Although a large part of each nasal is lost, the preserved lateralmost portions indicate transversely wide and anteroposteriorly long bones in dorsal view, but narrow in anterior view. Based on the preserved parts, a medial depression most likely excavated the anterodorsal surface of the joined nasals. Each nasal barely takes part to the corresponding premaxillary crest.

These specimens share many similarities with the holotype and only known specimen of *Khoikhoicetus agulhasis* SAM PQ 2678; the most salient are the rostral maxillary crest being dome-like, the medialmost angle of the right premaxillary sac fossa projecting medially towards the rounded medial edge of the left fossa, the medial margins of the right and left ascending processes converging slightly posterodorsally, the dorsal margin of each premaxillary crest sloping markedly ventrolaterally, and the large nasal on the vertex in dorsal view.

However, several differences are observed. In addition to their larger size (Table 1), the two Kerguelen specimens differ from SAM PQ 2678 in the following features:

1) The rostrum is distinctly triangular in dorsal view, with straight lateral edges; it is wider at its base and does not widen at mid-length as in SAM PQ 2678.

2) In anterior view, the premaxillary crests are distinctly wider than the premaxillary sac fossae, whereas they are significantly narrower in SAM PQ 2678. The condition on the right premaxillary crest of SAM PQ 2678 may be accentuated by wear and/or break of the lateralmost part; indeed, in anterior view and, as compared to the left side, the right crest seems truncated. Nevertheless, the difference is still valid for the left premaxillary crest, which is apparently unworn in SAM PQ 2678.

3) In lateral view, the premaxillary crests are located posterior to the premaxillary sac fossae, whereas in SAM PQ 2678 they are anteriorly projected and slightly overhang the premaxillary sac fossae.

4) In dorsal view, the bony nares are proportionally narrower and roughly oval-shaped, whereas they are wider and roughly circular in SAM PQ 2678. Because the three specimens of *Khoikhoicetus* are of different size, three measurements have been selected to establish comparable ratios for the relative width of the bony nares: the width between the premaxillary foramina (Wpf), the width between the main dorsal infraorbital foramina (Wdiof), and the length of the skull from the apex of rostrum to the posteriormost edge of the nasals (Pona). To establish the first two measurements, widths at lateral and medial edges of foramina have been measured, and the mean calculated has been used for Wpf and Wdiof. To establish the third measurement, we had to estimate the length of the rostrum of SAM PQ 2678, which is incomplete. The apex of the rostrum was reconstructed extending the lateral edges anteriorly, with a rounded end as in the two Kerguelen specimens (Fig. 4). This reconstruction suggests that about 30 mm are missing anteriorly. Therefore, the Pona of SAM PQ 2678 is the measurement taken from the specimen as preserved, to which we added 30 mm. Table 2 clearly establishes that the two specimens from Kerguelen Islands have relatively narrower bony nares compared to the holotype of *Khoikhoicetus agulhasis* and resemble each other in this respect more than they do the South African specimen.

5) The premaxillary sac fossae are proportionally significantly narrower than those of the holotype of *Khoikhoicetus agulhasis.* As for the relative width of the bony nares, the measurements of the width of the premaxillary sac fossae (Wpsf) of the three specimens have been compared on the basis of the three measurements mentioned above, Wpf, Wdiof, and Pona. Table 3 clearly establishes that the two specimens from Kerguelen Islands have relatively narrower premaxillary sac fossae than the holotype of *Khoikhoicetus agulhasis* and resemble each other in this respect more than they do the South African specimen.

and 6) The main dorsal infraorbital foramen of MNHN.F.COI. 1 and 13 is notably distant from the maxilla-premaxilla suture (from 10 to 20 mm), whereas it almost contacts this suture in SAM PQ 2678.

It may be tempting to interpret these differences as related to significant individual variation (ontogenetic and/or related to sexual dimorphism, as commonly observed in extant ziphiids). In order to evaluate if the disparity between the Kerguelen and South African specimens could be related to individual variation, we have referred to the variation observed in 10 specimens of the extant *Mesoplodon layardii* (Gray, 1865) and eight specimens of the extant *Mesoplodon densirostris* (Blainville, 1817) (Ross 1984: tables 8 and 25). We excluded from our sample the specimen of *M. layardii* mentioned by Ross (1984: table 8) as "Falkland Islands, Turner, 1880", which, given its size, is likely to be a juvenile, and the specimen of *M. densirostris* PEM1518/84 (Ross 1984: table 25), which is a foetus. We used two measurements provided by Ross (31 and 37), which correspond respectively to our width of the premaxillary sac fossae (Wpsf) and width of the bony nares (Wn). It is noteworthy that measurements of Ross (1984: tables 8 and 25) are expressed as percentages of the condylobasal length, a measurement not available for our specimens and replaced here by the length of the skull from the apex of rostrum to the posteriormost edge of nasals (Pona). However, this difference is likely to be of little incidence on our evaluation of the individual variation and on the comparison with our fossil sample. For the two extant species of *Mesoplodon* Gervais, 1850, we calculated the difference between the maximum and minimum value for each measurement and calculated the percentage of this difference to the minimum value. As observed in Table 4, the variation observed in our sample of *Khoikhoicetus* Bianucci, Lambert & Post, 2007 is much greater that in the two *Mesoplodon* species, especially in the case of the width of the premaxillary sac fossae, the disparity being less extreme in the case of the width of the bony nares. Because the variation observed in the three *Khoikhoicetus* specimens exceeds significantly that observed in two species of extant *Mesoplodon*, it is regarded here as related to interspecific rather that intraspecific variation. Clearly resembling each other more than they do the South African holotype of *Khoikhoicetus agulhasis*, the specimens from Kerguelen Islands are therefore referred to a new species of *Khoikhoicetus, K. kergueleni* n. sp.

Genus *Africanacetus* Bianucci, Lambert & Post, 2007

TYPE SPECIES. — *Africanacetus ceratopsis* Bianucci, Lambert & Post, 2007 by original designation.

OTHER REFERRED SPECIES. — *Africanacetus gracilis* Ichishima, Augustin, Toyofuku & Kitazato, 2017.

Africanacetus ceratopsis Bianucci, Lambert & Post, 2007

REFERRED SPECIMENS AND LOCALITIES. — Partial cranium MNHN.F.COI12 including rostrum, premaxillary sac fossae, part of both supraorbital regions, and vertex (Fig. 5); geographic coordinates 49°48'S, 66°28'E (Skiff Bank, SWW to Kerguelen Islands); depth 1680 m. Partial cranium MNHN.F.COI2 including rostrum, premaxillary sac fossae, and part of both supraorbital regions (Fig. 6); geographic coordinates 47°07'58.8"S, 65°44'59.4"E (290 km NW to Kerguelen Islands); depth 1622 m (Fig. 1).

BRIEF DESCRIPTION AND COMPARISON

The rostrum is not complete anteriorly in both specimens, although it is probably close to the original length in MNHN.F.COI2. Probably half of the rostrum in missing in COI12. The rostrum is robust and nearly as wide as high at half of its preserved length on COI2. The mesorostral groove is completely filled with the vomer, the latter reaching a dorsal level much higher than the bordering premaxilla. A median suture is visible on the dorsal surface along the proximal part of the vomer on COI2. The lateral margin of the rostrum of COI2 is a sharp crest in its proximal part; this crest forms a thin blade markedly diverging towards the prominential notch; the blade is somewhat thicker on the left side. No crest is observed on COI12 (except at the rostrum base, close to the prominential notch) and in dorsal view the rostrum is significantly narrower and more slender than on the other specimen. In lateral view, no indication for individual alveoli could be found on the maxilla. Deeper on COI12, the prominential notch is followed posteriorly by a dome-shaped, moderately elevated rostral maxillary crest (*sensu* Mead & Fordyce 2009). The crest is higher and more posteriorly located on the right side. Compared to COI2, right and left crests are more elevated, massive, and rounded on COI12. A small dorsal infraorbital foramen is present at the top of each crest (on COI2) and a large foramen pierces the medial base of the crest, being followed anteriorly by a shallow depression. Anterolateral to the rostral maxillary crest, the antorbital notch is widely open anteriorly, barely limited laterally by a short anterior extension of the antorbital part of the maxilla and the lacrimojugal complex. Medial to the antorbital notch a small maxillary tubercle protrudes anteriorly. The maxillary tubercle is more salient in COI12, in relation to the larger maxillary crest in this specimen. Right and left premaxillary foramina are difficult to distinguish, hidden by a concretion. Each premaxillary sac fossa is thick, with the dorsal surface raising dorsomedially.

The ascending process of the premaxilla of MNHN.F.COI12 strongly raises dorsally, with its anterior surface being almost subvertical when reaching the level of the premaxillary crest. Each ascending process is distinctly constricted transversely at the level of the maximum width of the bony nares. The vertex is well preserved on COI12, with intact premaxillary crests. The latter are robust and the right crest diverges posterolaterally, whereas the left crest is directed more laterally. In dorsal view, the nasals are anteroposteriorly long and transversely wide; their anterolateral angle reaches the medial margin of the corresponding premaxillary crest, without being integrated in it. In dorsal view, the median suture of the nasal is salient anteriorly, dorsal to the presphenoid.

The thick vomer in the mesorostral groove, the dome-like rostral maxillary crest, and the dorsomedially raising premaxillary sac fossae are similarly observed in specimens of *Africanacetus ceratopsis* from South Africa (Bianucci *et al.* 2007). The dimensions of the rostrum and facial region (Table 5) match well the South African sample of *A. ceratopsis* and the specimens of *Africanacetus* sp. from the Banzare Bank, southernmost part of the Kerguelen Plateau, described by Gol'din & Vishnyakova

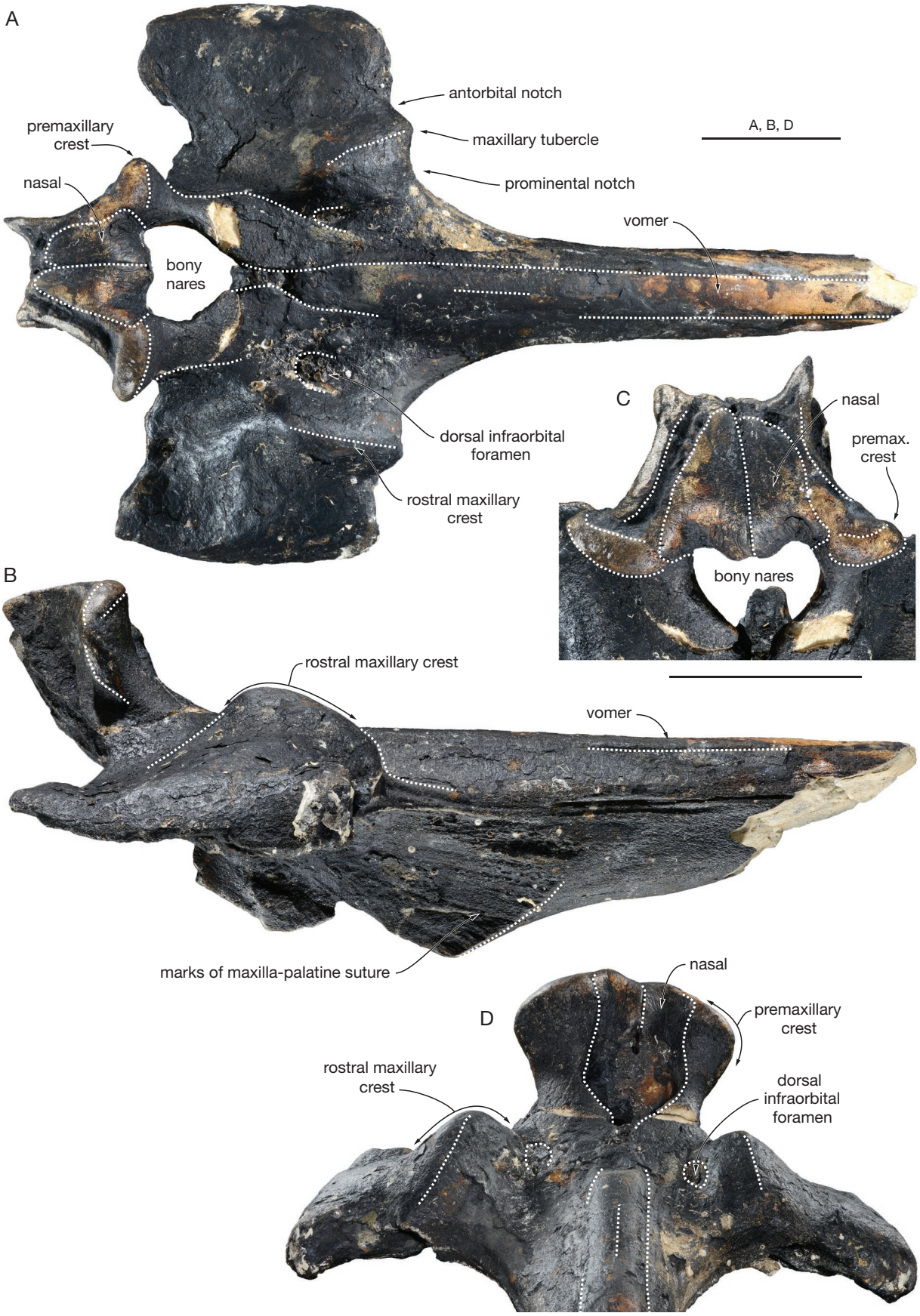

Fig. 5. — Partial cranium of *Africanacetus ceratopsis* (MNHN.F.COI12): **A**, dorsal view; **B**, right lateral view; **C**, detail of the vertex in dorsal view; **D**, anterodorsal view. Scale bars: 100 mm.

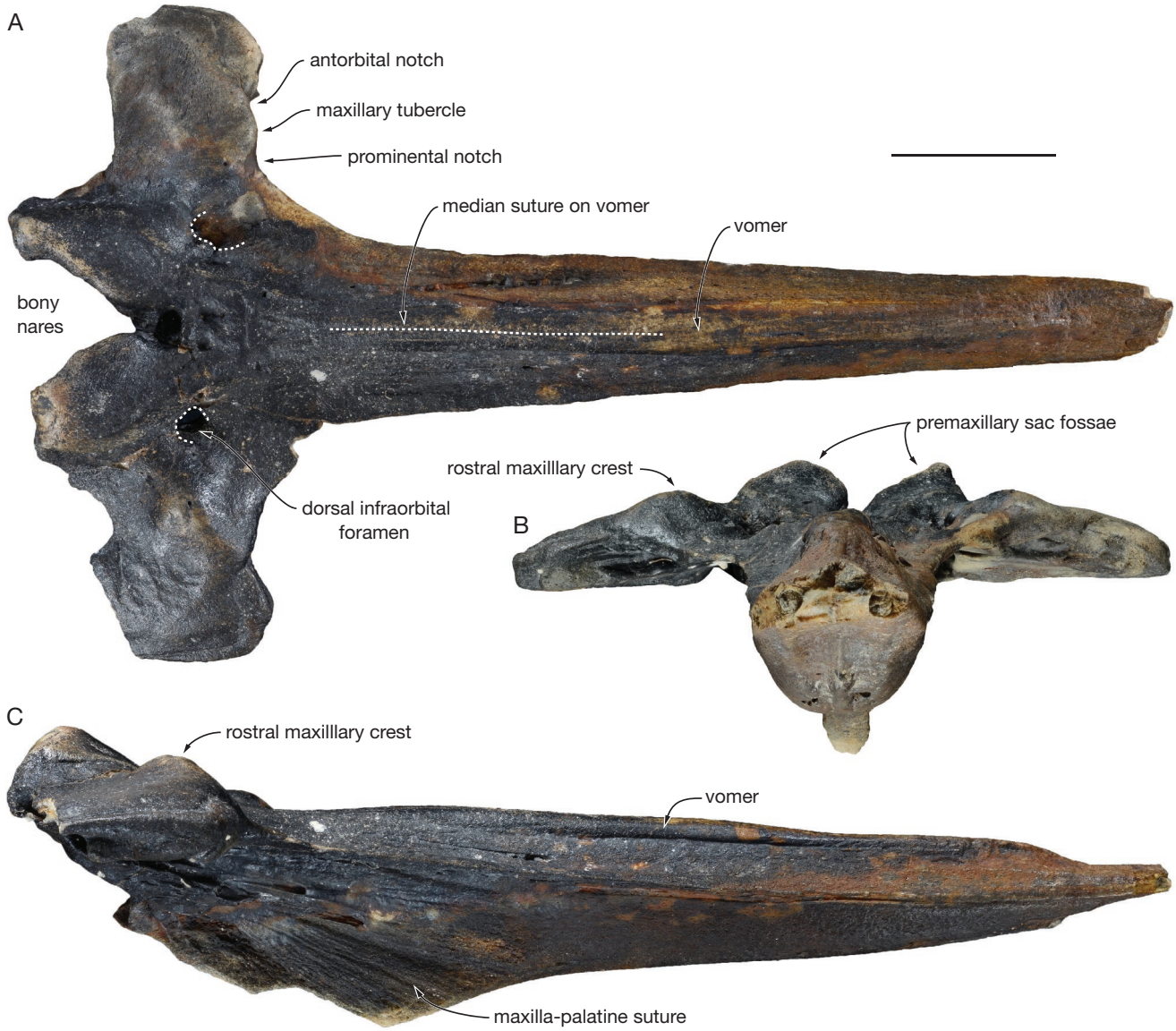

Fig. 6. — Partial cranium of *Africanacetus ceratopsis* Bianucci, Lambert & Post, 2007 (MNHN.F.COI2): **A**, dorsal view; **B**, anterior view; **C**, right lateral view. Scale bar: 100 mm.

(2012). The rostral maxillary crests are significantly lower on MNHN.F.COI2 and more rounded on MNHN.F.COI12. For part of the dimensions, the holotype of *Africanacetus gracilis* is moderately to markedly smaller, especially for the measurements at rostrum base (see Ichishima *et al.* 2017). As in the latter, the antorbital notch of both specimens is more anteriorly located than in the holotype of *A. ceratopsis* and several referred specimens; such differences may be explained by sexual dimorphism or any other intraspecific, population-related morphological variation.

Hyperoodontinae indet. aff. *Africanacetus*

Referred specimens and localities. — Partial rostrum MNHN.F.COI3. Partial rostrum MNHN.F.COI4 (Fig. 7). These specimens were collected before the involvement of procedures to record localities; no indication about the precise locality is thus available. They were most likely found off Kerguelen Islands.

Brief description and comparison

In dorsal view these two robust rostra display a minor constriction slightly posterior to mid-length, followed anteriorly by a distinct widening. The acute lateral margin of the rostrum forms a plate diverging abruptly posterolaterally. The vomer is widely exposed dorsally in the mesorostral groove, and is margined by longitudinal sulci along its anterior portion. Posterior to the vomer, the presphenoid is similarly thickened in the mesorostral groove, raising posteriorly until the level of the premaxillary foramen. The premaxillary foramen is at the same anteroposterior level as the large dorsal infraorbital foramen, posterior to the anterior tip of the presphenoid.

FIG. 7. — Partial rostra of Hyperoodontinae indet. aff. *Africanacetus*: **A**, **B**, MNHN.F.COI3; **C**, **D**, MNHN.F.COI4; **A**, **C**, dorsal views; **B**, **D**, right lateral views. Scale bar: 100 mm.

A lateral expansion of the rostrum, as seen in dorsal view of these two specimens, is absent in *Africanacetus ceratopsis*, but present in *Pterocetus benguelae* (holotype and SAM PQ 69684) and *Africanacetus gracilis* (Ichishima *et al.* 2017). Specimens of *P. benguelae* similarly display a wide exposure of the vomer in the mesorostral groove, with a pointed anterior portion margined by sulci (e.g. SAM PQ 1770 and 69684). However, in *P. benguelae* the premaxillary foramen is much more anteriorly located, anterior to the large dorsal infraorbital foramen. The absence of this key character in MNHN.F.COI3 and MNHN.F.COI4 makes these two rostra slightly more similar to *A. ceratopsis* than to *P. benguelae*. The rostrum of *A. gracilis* is considerably more slender. More robust than currently known specimens of *A. ceratopsis* these two rostra are too incomplete for a more precise taxonomic assignation.

TABLE 5. — Measurements (in mm) on the partial crania of *Africanacetus ceratopsis* Bianucci, Lambert & Post, 2007 (MNHN.F.COI2, COI12, and NMR 991-00001993 [holotype] [from Bianucci *et al.* 2007]). Abbreviations: +, not complete; –, no data.

Africanacetus ceratopsis	MNHN.F.COI2	MNHN.F.COI12	NMR 991-00001993 (holotype)
Rostrum length	+586	–	+475
Height of rostrum at mid-length as preserved	89	–	–
Width of rostrum at mid-length as preserved	82	–	–
Maximum opening of mesorostral groove	32	37	38
Width of rostrum at base (level prominential notch)	–	190	–
Width of rostrum at base (level antorbital notch)	294	275	–
Preorbital width	420	422	–
Width of premaxillary sac fossae	155	127	161
Width of right premaxillary sac fossa	+74	61	78
Width of left premaxillary sac fossa	+63	54	61
Width of bony nares	–	67	72
Minimum width of right ascending process of premaxilla	–	33	–
Width of premaxillary crests	–	165	187
Width of right premaxillary crest	–	64	83
Width of left premaxillary crest	–	43	52
Minimum distance between premaxillary crests	–	79	63
Maximum width of nasals	–	79	70
Length of medial suture between nasals	–	65	60
Minimum posterior distance between maxillae	–	44	63

Genus *Mesoplodon* Gervais, 1850

Mesoplodon sp. aff. *Mesoplodon layardii* (Gray, 1865)

REFERRED SPECIMENS AND LOCALITIES. — Partial cranium MNHN.F.COI5 including rostrum and right supraorbital region (Fig. 8A-C); geographic coordinates 48°08'43.8"S, 71°59'13.8"E (150 km NE to Kerguelen Islands); depth 1720 m (Fig. 1). Partial cranium MNHN.F.COI6 including rostrum and right supraorbital region (Fig. 8D-E); geographic coordinates 45°53'49.2"S, 67°19'40.8"E (330 km NNW to Kerguelen Islands); depth 1959 m (Fig. 1). Rostrum fragment MNHN.F.COI7 (Fig. 8F); geographic coordinates 44°54'39.6"S-44°25'30.0"E (445 km W to Crozet Islands); depth 1222 m (Fig. 1).

BRIEF DESCRIPTION AND COMPARISON

The general aspect of the bone of these three specimens is markedly different from other cranial remains of the sample; the bone is whiter, less compact, and more crumbly in the outer regions. The ventral surface of the rostrum in these three specimens is more damaged than the dorsal surface, a condition most likely due to the presence of more spongy bone ventrally, as observed via computed tomography in several extant ziphiids (Lambert *et al.* 2011).

The rostrum is elongated, being incomplete anteriorly at least in MNHN.F.COI7 and COI6; it is higher than wide at estimated mid-length (Table 6). The mesorostral groove is completely filled with the vomer. The latter is especially dorsally inflated in the proximal region of the rostrum, with a visible median suture. Towards mid-length, the dorsal exposure of the vomer narrows markedly, concomitantly to a conspicuous lowering of its height above the premaxilla as seen in lateral view (Fig. 8C, E, F). The lateral margin of the rostrum diverges only slightly towards the corresponding antorbital notch. The maxilla-premaxilla suture approaches the lateral margin of the rostrum at a level 100-150 mm anterior to the antorbital notch, whereas a transverse constriction of the premaxilla occurs in front of the notch. One large dorsal infraorbital foramen is opening anterolaterally at a level posterior to the antorbital notch. An anteriorly directed, smaller dorsal infraorbital foramen is located medial to the notch in MNHN.F.COI7 and COI5. Slightly posterior to level of antorbital notch, the premaxillary foramen is anterior to the large dorsal infraorbital foramen and located higher dorsally than the latter. There is no rostral maxillary crest and no conspicuous maxillary crest posterolateral to the antorbital notch, the supraorbital region being low and roughly flat, with only a slight elevation of the dorsal surface of the maxilla just anterior to the posterior dorsal infraorbital foramen. Although only the maxilla is preserved in that region, the anteromedial corner of the right bony naris displays a distinct elevation.

Among extinct and extant hyperoodontines, apart from the considerably flatter supraorbital region lacking any high crest, these three fragmentary cranial remains share the highest number of similarities with the strap-toothed whale *Mesoplodon layardii* for the narrow and high rostrum, the markedly inflated vomer in the proximal part of the mesorostral groove, the topology of the foramina in the rostrum base area, and the elevation of the right anteromedial corner of the bony nares (see Turner 1880; Hale 1931). Even more strikingly, the narrowing of the dorsal exposure of the vomer towards mid-length of rostrum and the related lowering of its height are similarly observed to various extents in specimens of *M. layardii*, where this region is surrounded by the greatly enlarged and posterodorsomedially curved lower tusks in adult males (e.g. SAM 38236, 40479, USNM 550150; Van Beneden & Gervais 1880: pl. 27; Mead 1989a: fig. 15I; Fig. 9).

Comparing measurements of these three specimens with skulls of *Mesoplodon layardii* (sample of 11 specimens, including males and females, from Australia, Falkland

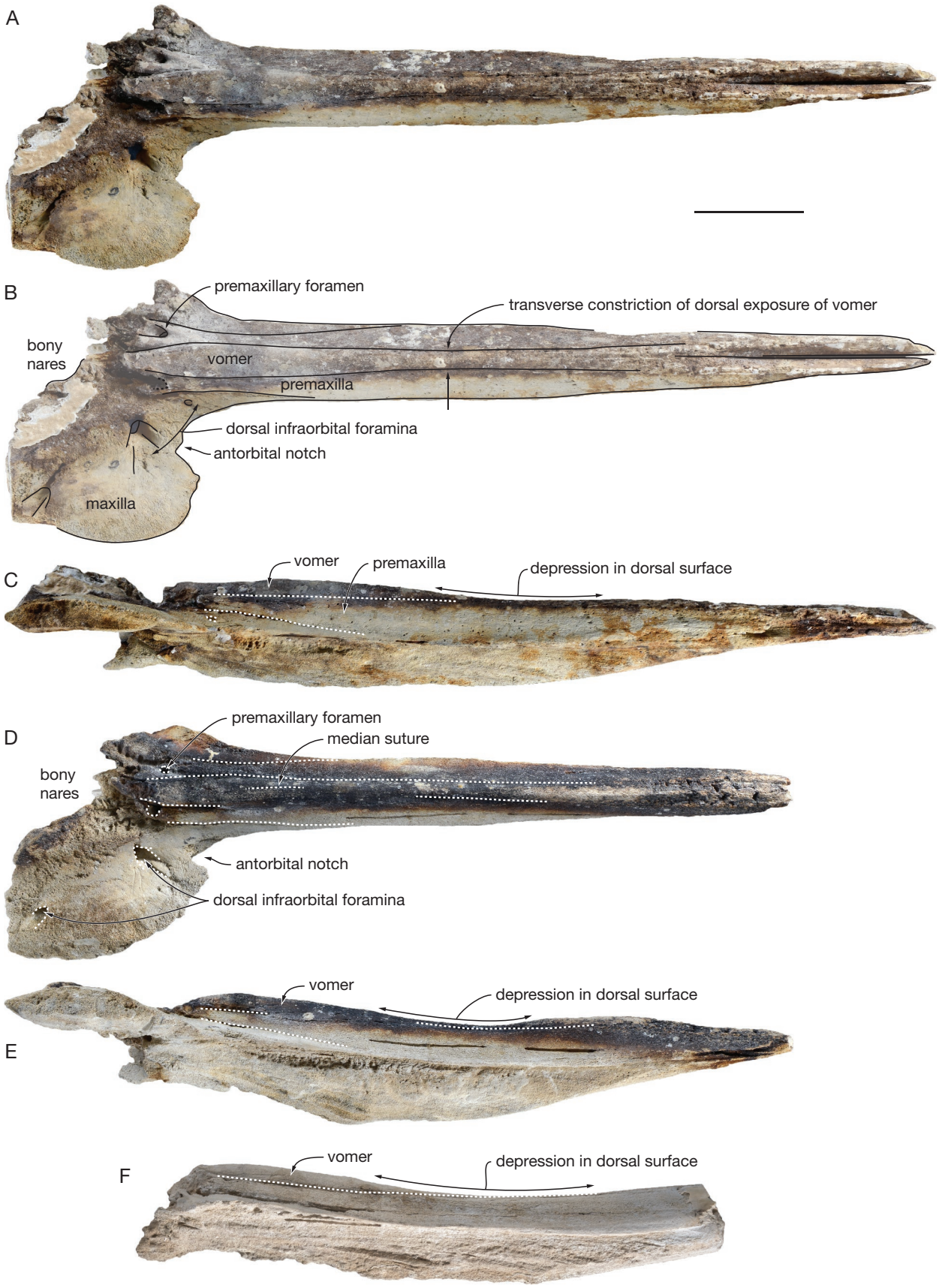

FIG. 8. — Partial crania of *Mesoplodon* sp. aff. *Mesoplodon layardii*: **A**-**C**, MNHN.F.COI5; **D**-**E**, MNHN.F.COI6; **F**, MNHN.F.COI7; **A**, **B**, **D**, dorsal views; **C**, **E**, **F**, right lateral views. Scale bar: 100 mm.

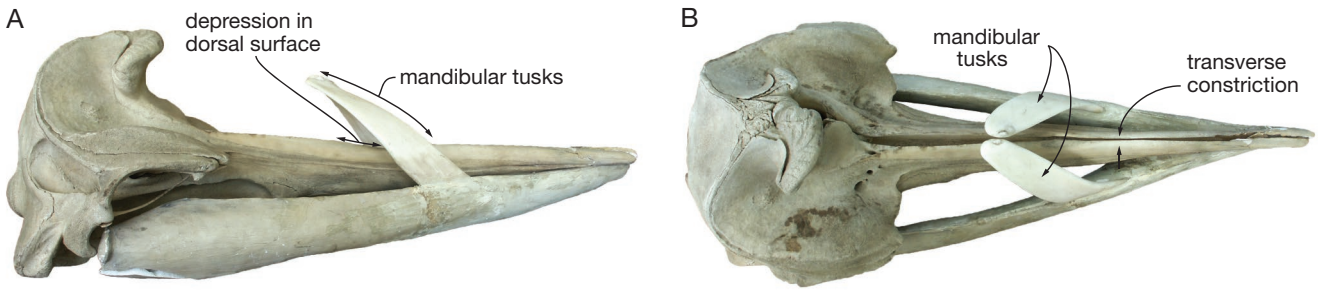

FIG. 9. — Skull of the extant strap-toothed whale *Mesoplodon layardii* (unnumbered SAM specimen) showing the relationship between the large mandibular tusks, the depression in the dorsal surface of the rostrum, and the transverse constriction of the dorsal opening of the mesorostral groove. Note that except for the tusks the mandibles are made of plaster, and that the tusks are positioned slightly too posterior along the rostrum as compared to their *in vivo* position. Photos by G. Bianucci.

TABLE 6. — Measurements (in mm) on the partial crania of *Mesoplodon* sp. aff. *Mesoplodon layardii* (MNHN.F.COI5, MNHN.F.COI6, and MNHN.F.COI7). Abbreviations: **e**, estimate; **+**, not complete; **–**, no data.

Mesoplodon* sp. aff. *M. layardii	**MNHN.F.COI5**	**MNHN.F.COI6**	**MNHN.F.COI7**
Total length as preserved	880	738	557
Rostrum length as preserved	e703	560	468
Distance between left premaxillary foramen and apex of rostrum as preserved	716	588	492
Width of anterior section of rostrum	–	–	48
Height of anterior section of rostrum	–	–	67
Width of rostrum at estimated mid-length	66	+60	–
Height of rostrum at estimated mid-length	76	87	–
Maximum height of rostrum	+99	+118	+90
Maximum width of vomer in dorsal view	29	31.5	32
Maximum height of vomer above premaxilla	17	14	15.5
Distance between left premaxillary foramen and lowest and narrowest region of the vomer in the mesorostral groove	e310	e280	e270
Height of rostrum at lowest level of vomer	+83	93	–
Transverse diameter of left/right premaxillary foramina	5.5/–	6.3/e6.5	e8/–
Distance between anterior tips of premaxillary foramina	e44	37.5	e44
Width of premaxillae at level of anterior tip of premaxillary foramen	e67	+65	+62
Supraorbital width of the maxilla	e340	e310	–
Diameter of large right dorsal infraorbital foramen	19	13	–

Islands, and South Africa in Ross 1984), a few differences are noted. The general dimensions of the three specimens are smaller than large adults of *M. layardii*. The ratio between estimated postorbital width and rostrum length is distinctly lower in MNHN.F.COI5, corresponding to a proportionally longer rostrum, whereas the ratio falls in the lower part of the range of *M. layardii* for the incomplete rostrum COI6. The width and height at mid-length of the rostra COI5 and COI6 are in the upper part of the range for *M. layardii*, corresponding to a proportionally greater cross section in line with the relatively longer rostrum. Pending the discovery of more complete specimens and/or the extraction of ancient DNA (see discussion on geochronological age below), these three specimens are identified as *Mesoplodon* sp. aff. *M. layardii*.

Interestingly, an isolated, poorly preserved ziphiid rostrum found on a beach of Kerguelen Islands and tentatively attributed (Robineau 1973) to the extant Andrew's beaked whale *Mesoplodon bowdoini* shares some similarities with the specimens described here. Characterized among other features by its great length, this beached rostrum may correspond to the same taxon.

Subfamily ZIPHIINAE Gray, 1850 *sensu* Bianucci *et al.* (2016)

Genus *Izikoziphius* Bianucci, Lambert & Post, 2007

TYPE SPECIES. — *Izikoziphius rossi* Bianucci, Lambert & Post, 2007 by original designation.

OTHER REFERRED SPECIES. — *Izikoziphius angustus* Bianucci, Lambert & Post, 2007.

Izikoziphius rossi Bianucci, Lambert & Post, 2007

REFERRED SPECIMEN AND LOCALITY. — Partial cranium MNHN.F.COI8 including rostrum, premaxillary sac fossae, and vertex (Fig. 10); geographic coordinates 49°50'44.4"S, 63°19'27.6"E (Skiff Bank, 390 km SWW to Kerguelen Islands); depth 2041 m (Fig. 1).

BRIEF DESCRIPTION AND COMPARISON

The cross section of the long and robust rostrum (not complete apically) is considerably wider than high for most of the rostral length (Table 7). A marked dorsal and lateral expansion of the thickened lateral margin of the rostrum has a maximum extent

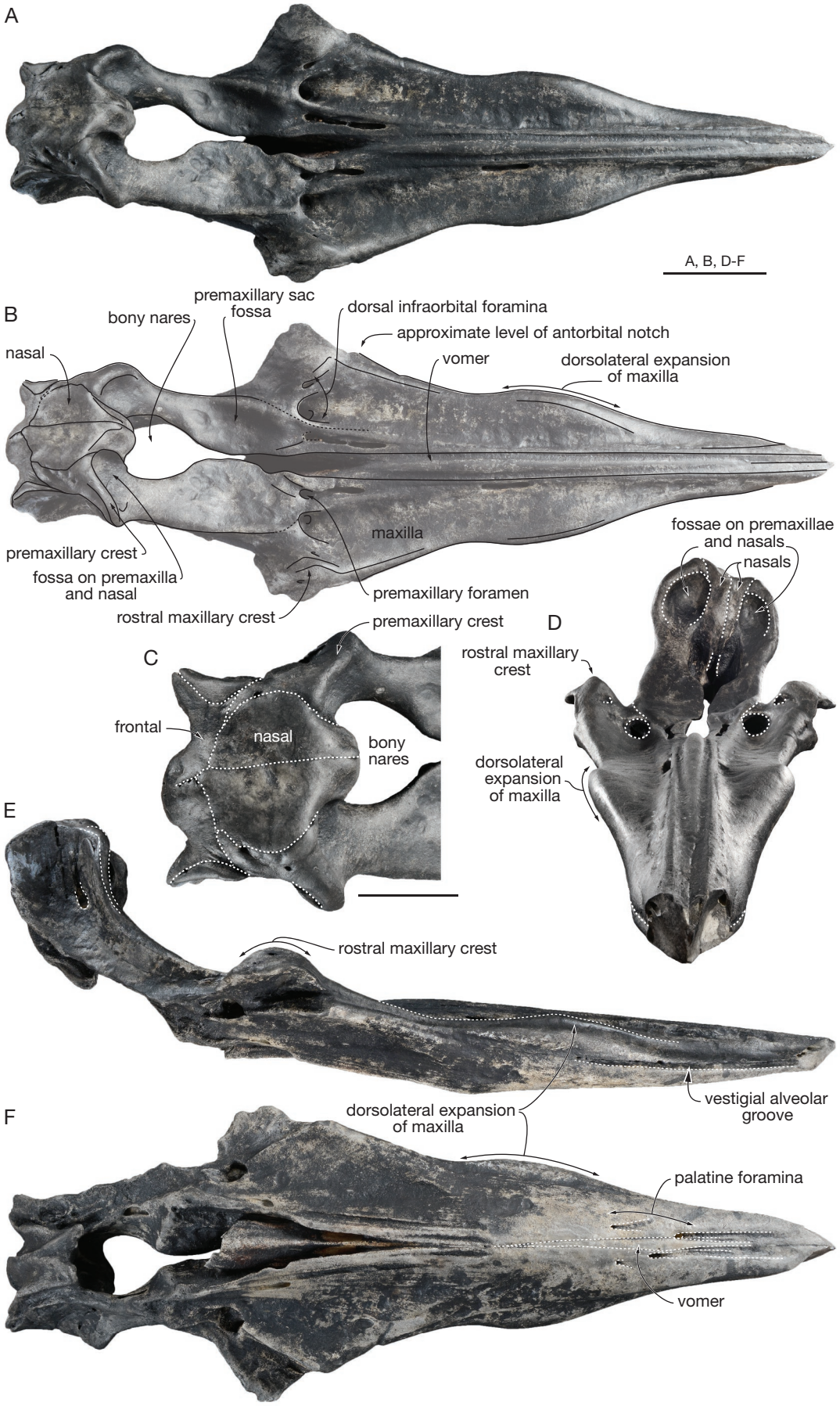

FIG. 10. — Partial cranium of *Izikoziphius rossi* (MNHN.F.COI8): **A**, dorsal view; **B**, same view with interpretive line drawing; **C**, detail of the vertex in dorsal view; **D**, anterodorsal view; **E**, right lateral view; **F**, ventral view. Scale bars: A, B, D-F, 100 mm; C, 50 mm.

TABLE 7. — Measurements (in mm) on the partial crania of *Izikoziphius rossi* (MNHN.F.COI8, PEM N 3265, and SAM PQ 2086 [from Bianucci *et al.* 2007]). Abbreviations: **e**, estimate; **+**, not complete; **–**, no data.

Izikoziphius rossi	MNHN.F. COI8	PEM N 3265 (holo.)	SAM PQ 2086
Rostrum length	e495	+490	e530
Height of rostrum at mid-length	72	+100	84
Width of rostrum at mid-length	106	115	94
Maximum width of rostrum at dorsolateral expansion	155	–	–
Width of premaxillary sac fossae	131	145	155
Width of right premaxillary sac fossa	72	75	80
Width of left premaxillary sac fossa	58	55	62
Width of bony nares	60	56	73
Minimum width of right ascending process of premaxilla	48	–	45
Width of premaxillary crests	147	129	+126
Width of right premaxillary crest	45	71	–
Width of left premaxillary crest	36	32	–
Minimum distance between premaxillary crests	54.5	–	69
Maximum width of nasals	83	–	e88

at about mid rostral length, resulting in the lateral margin of the rostrum being distinctly convex in dorsal view in that region. The mesorostral groove is filled by the thickened vomer until the level of the antorbital notches, and the dorsal surface of the vomer is transversely concave in the apical part of the rostrum. On the ventral surface of the rostrum, lateral to the ventral exposure of the vomer the maxillae are pierced by several large palatal foramina, anteriorly followed by deep sulci. The rostrum is broad at its base, with a depressed medial region laterally margined by the rostral maxillary crest. The latter progressively raises past the antorbital notch level, forming a high hump in the antorbital region, best seen in lateral view. Medial to the rostral maxillary crest, a large dorsal infraorbital foramen is followed anteriorly by a wide depression. Several smaller foramina pierce the rostral maxillary crests. The premaxillary foramen is roughly in line with the large dorsal infraorbital foramen, both being posterior to the estimated level of the antorbital notch. The two premaxillary sac fossae are moderately transversely concave, and the right fossa is distinctly wider than the left (Table 7). The lateral margin of each ascending process of the premaxilla is moderately constricted in anterior view.

The vertex of the cranium is elevated, with the anterior surface of the ascending process of the premaxilla reaching the vertical. This anterior surface is excavated on both sides by a deep fossa, extending somewhat on the lateral part of the corresponding nasal. Each premaxillary crest is directed anterolaterally, and the right crest is wider and dorsally higher than left crest.

Both nasals are longer than wide, extending anteriorly beyond the level of the corresponding premaxillary crest. The right nasal is significantly longer posteriorly than the left. From their anterior apices, the lateral margins of the right and left nasals diverge abruptly until mid-length. The median region of the dorsal surface of the nasals is depressed.

The combination of a mesorostral groove filled with the vomer, a high vertex with anterolaterally directed premaxillary crests, and anteriorly elongated nasals point to a ziphiine attribution (*sensu* Bianucci *et al.* 2016). Other characters (e.g. the long rostrum, the absence of a prenarial basin, the fossa on the anterior surface of the ascending process of the premaxilla, and the relatively long contact between nasal and premaxilla) contrast with *Ziphius* (adult males of the latter for the prenarial basin) and unambiguously indicate affinities with *Izikoziphius*. Within the latter genus, MNHN.F.COI8 shares several characters with *Izikoziphius rossi*: rostrum wider than high at mid-length, rostral maxillary crest extending on rostrum base, large fossa on the anterior surface of the ascending process of the premaxilla extending on the corresponding nasal, median depression of the dorsal surface of the nasals, and right premaxillary crest much higher than left crest.

However, MNHN.F.COI8 differs from the two currently known specimens of *I. rossi* in the marked dorsolateral expansion of the lateral margin of the rostrum at mid-length. Pending the discovery of additional specimens this conspicuous difference is interpreted here as intraspecific variation, maybe indicating sexual dimorphism as recorded in several extant ziphiids and inferred in a few extinct species (Heyning 1989; Mead 1989b; Bianucci *et al.* 2013). It could nevertheless also indicate a closely related new species of *Izikoziphius*.

Interestingly, although much less developed this expansion of the lateral margin of the rostrum is to some degree reminiscent of the huge rostral maxillary crests observed in SAM PQ 2717 and 2719, two specimens from the South African fauna(s) previously attributed to Odontoceti indet. due to their fragmentary state of preservation (Bianucci *et al.* 2007). In addition to rostral maxillary crests with the same position and orientation as the expansion of the lateral margin of the rostrum in MNHN.F.COI8, SAM PQ2717 and 2719 share with the latter a thickened vomer in the mesorostral groove, the dorsal surface of the vomer being transversely concave in the apical region of the rostrum, and several large palatal foramina. Together with the high compactness of rostral bones, all these similarities point to ziphiid (and maybe even ziphiine) rather than physeterid affinities for these two mysterious specimens (G. Bianucci pers. comm. 2017).

Genus *Ziphius* Cuvier, 1823

Ziphius sp.
(probably new species)

Ziphius sp. – Bianucci *et al.* 2007: 576; 2008: 141.

REFERRED SPECIMEN AND LOCALITY. — Fragment of the facial region of the cranium MNHN.F.COI9 including right premaxillary sac fossa and most of the vertex (premaxillary crests and nasals) (Fig. 11). This specimen was collected before the involvement of procedures to record localities; no indication about the precise locality is thus available. It was most likely found off Kerguelen Islands.

BRIEF DESCRIPTION AND COMPARISON

Only preserved on the right side, the premaxillary sac fossa is transversely and longitudinally concave. In anterior view the

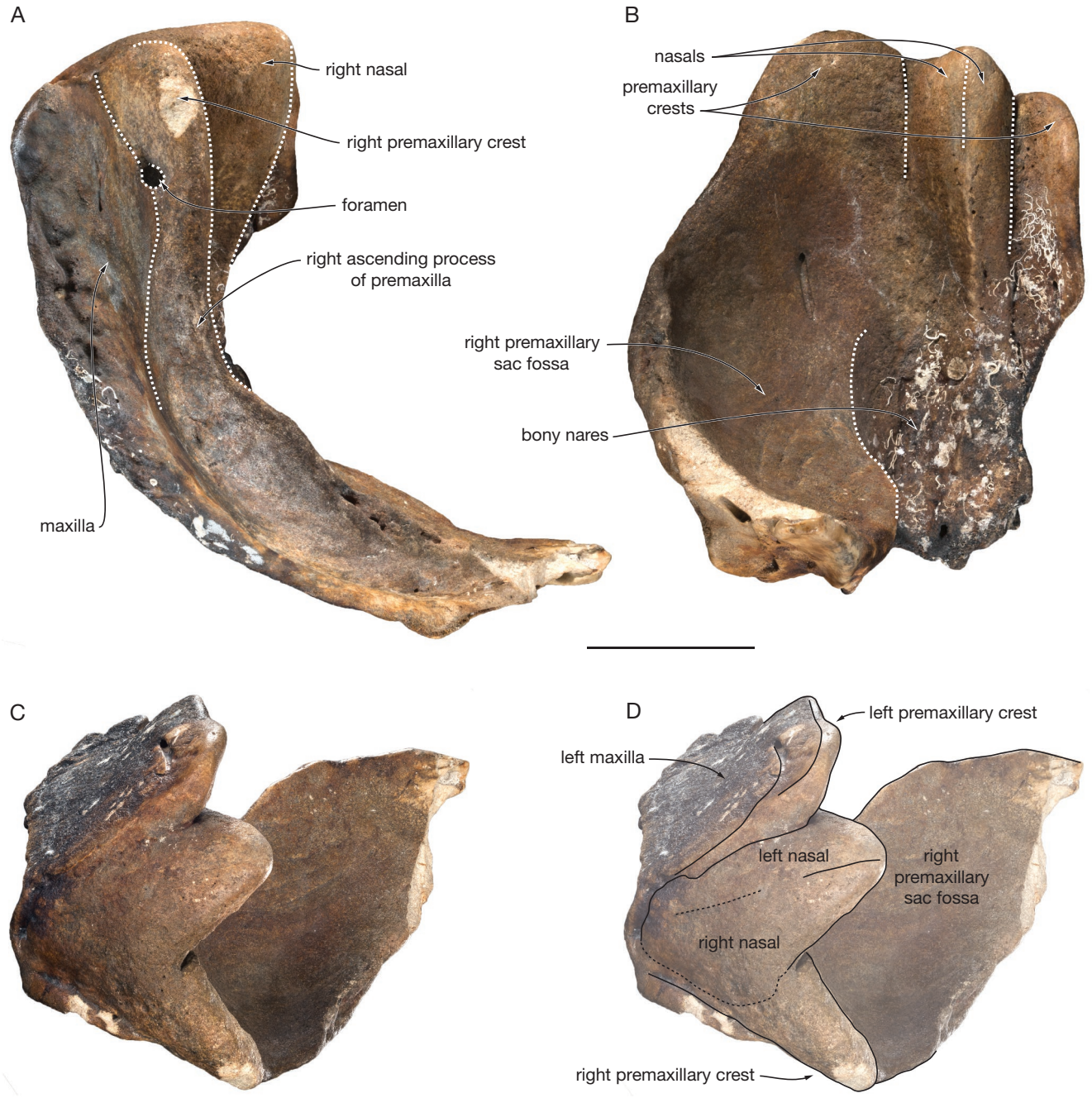

FIG. 11. — Fragment of facial region of the cranium of *Ziphius* sp. (probably new species) (MNHN.F.COI9): **A**, right lateral view; **B**, anterior view; **C**, dorsal view; **D**, same view with interpretive line drawing. Scale bar: 100 mm.

TABLE 8. — Measurements (in mm) on the fragments of facial region of the cranium of *Ziphius* sp. (MNHN.F.COI9 and SAM PQ 2826 [from Bianucci *et al.* 2007]). Abbreviations: **e**, estimate; **+**, not complete; **–**, no data.

***Ziphius* sp.**	**MNHN.F. COI9**	**SAM PQ 2826**
Width of right premaxillary sac fossa	153	+141
Width of right bony naris	e71	–
Width of right premaxillary crest	82	79
Width of left premaxillary crest	49	–
Maximum width of nasals	e67	76
Length of medial suture between nasals	150	149
Minimum posterior distance between maxillae	e51	–

lateral margin of the ascending process of the premaxilla does not display a conspicuous constriction. The right ascending process is much wider than the left process (preserved in its upper region), and the anterior surface of each process is transversely concave. On the elevated vertex, the anterolaterally directed right premaxillary crest is much wider than the left crest, the latter being even more anteriorly directed. A vertical foramen pierces the posterior flank of each crest at the boundary between premaxilla and maxilla. In dorsal view the nasals are anteroposteriorly elongated, much longer than wide. Their anteromedial apex projects farther

anteriorly than the premaxillary crests. The minimum distance between maxillae across the vertex is lower than the maximum width of nasals.

All the features listed above are shared with the extant *Ziphius cavirostris* Cuvier, 1823, more specifically adult males who display markedly transversely concave premaxillary sac fossae in the deep prenarial basin (e.g. True 1910; Heyning 1989). The latter only differs in being considerably smaller in general dimensions. Interestingly, this fossil specimen shares morphological characters and dimensions with the South African specimen of *Ziphius* sp. SAM PQ 2826 (Table 8). Furthermore, these two fossils nearly exactly preserve the same cranial regions, which may be an indication of a similar distribution of compact bone in the cranium (see a CT scan of the cranium of *Z. cavirostris* in Lambert *et al.* 2011: fig. 8). Although these two specimens represent a very large, new ziphiine species closely related to *Ziphius cavirostris*, their fragmentary state does not allow for a detailed differential diagnosis. Pending the discovery of more complete specimens, we therefore prefer not to define and name the new species.

Table 9. — Measurements (in mm) on the partial crania of *Xhosacetus hendeysi* (MNHN.F.COI10 and SAM PQ 2082 [holotype] [from Bianucci *et al.* 2007]). Abbreviations: **e**, estimate; **+**, not complete; **–**, no data.

Xhosacetus hendeysi	MNHN.F. COI10	SAM PQ 2082 (holotype)
Rostrum length	+447	+435
Height of rostrum at mid-length	78	–
Width of rostrum at mid-length	68	–
Maximum opening of mesorostral groove	36.5	33
Width of rostrum at base	140	187
Width of premaxillae at rostrum base	e65	–
Preorbital width	306	e330
Width of premaxillary sac fossae	129	119
Width of right premaxillary sac fossa	59.5	59
Width of left premaxillary sac fossa	52	51
Width of bony nares	65	61
Minimum width of right ascending process of premaxilla	29	29
Minimum width of left ascending process of premaxilla	22	–
Width of premaxillary crests	154	138
Width of right premaxillary crest	54	43
Width of left premaxillary crest	49	40
Minimum distance between premaxillary crests	54	53
Maximum width of nasals	66.5	65
Maximum width of right nasal	36.5	–
Maximum width of left nasal	30	–

Ziphiidae subfamily indet.

Genus *Xhosacetus* Bianucci, Lambert & Post, 2007

Type and only referred species. — *Xhosacetus hendeysi* Bianucci, Lambert & Post, 2007 by original designation.

Xhosacetus hendeysi Bianucci, Lambert & Post, 2007

Referred specimen and locality. — Partial cranium MNHN.F.COI10 including rostrum, facial region, and vertex (Fig. 12); geographic coordinates 48°00'42.0"S, 65°34'09.6"E (255 km NWW to Kerguelen Islands); depth 1145 m (Fig. 1).

Brief description and comparison

The apex of the rostrum of this well-preserved specimen is incomplete. The mesorostral groove is completely filled with the vomer. The dorsal surface of the latter becomes progressively keeled from mid-length of the rostrum in the posterior direction and a longitudinal sulcus marks the right and left vomer-premaxilla contacts. A median suture is visible on the posterior half of the vomer in the mesorostral groove. The vomer-presphenoid suture is transversely directed, located at a level posterior to the premaxillary foramen. Deep longitudinal openings on the lateral surfaces of the rostrum most likely result from partial wear of superior alveolar canals. The shallow groove appearing ventral to these openings in the anterior half of the rostrum is probably a vestigial alveolar groove. The lateral margin of the rostrum raises posterodorsolaterally, forming a robust ridge that laterally defines a medial depressed area made of the premaxillae and vomer. No distinct prominential notch being present, the ridge joins the elevated, dome-like rostral maxillary crest, the latter being posterior and slightly medial to the widely open and relatively deep antorbital notch. The right rostral maxillary crest is transversely narrower than the left, slightly higher, and extends more posteriorly. A large dorsal infraorbital foramen is anteromedial to each rostral maxillary crest.

The premaxillary foramen is located at the level of the antorbital notch, and the dorsal surface of anteriormost portion of the premaxillary sac fossa slopes anteromedially. At its maximum width, the premaxillary sac fossa is transversely concave. The relatively short ascending process of premaxilla displays an abrupt elevation, with its anterior surface becoming roughly vertical in its upper part; the left process is slightly less erected. Right and left ascending processes display a strong transverse constriction as seen in anterior view. Each premaxillary crest is directed laterally and slightly posterolaterally, with a curve more pronounced on the slightly longer right crest. The nasals occupy a large area on the vertex, with the right nasal longer and wider than the left. The anteromedial tip of the joined nasals reaches the same anteroposterior level as the anterior margin of the premaxillary crests. The anterodorsal margin of each nasal is excavated by a wide, subvertical groove, best seen in dorsal view. The dorsal surface of the nasals displays a slight medial depression and anteromedial slope. The contribution of each nasal to the corresponding premaxillary crest is minor.

In addition to similar dimensions (Table 9), this specimen shares many features with the holotype of *Xhosacetus hendeysi*, including the size and shape of the nasals on the vertex, the morphology of the premaxillae in the facial region, the developed rostral maxillary crests (erroneously named maxillary crests and premaxillary crests in different

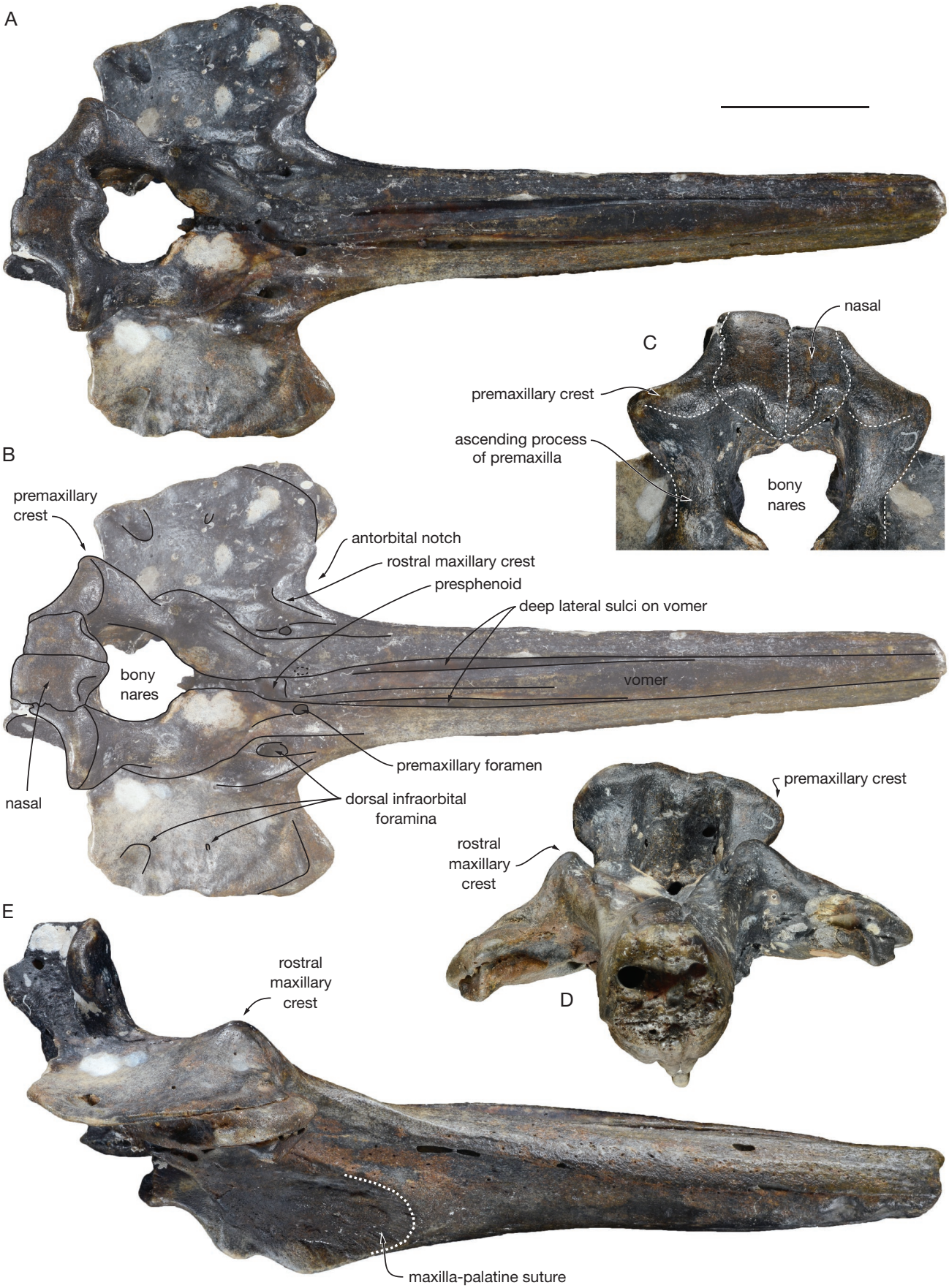

FIG. 12. — Partial cranium of *Xhosacetus hendeysi* (MNHN.F.COI10): **A**, dorsal view; **B**, same view with interpretive line drawing; **C**, detail of the vertex in dorsal view; **D**, anterior to slightly anterodorsal view; **E**, right lateral view. Scale bar: 100 mm.

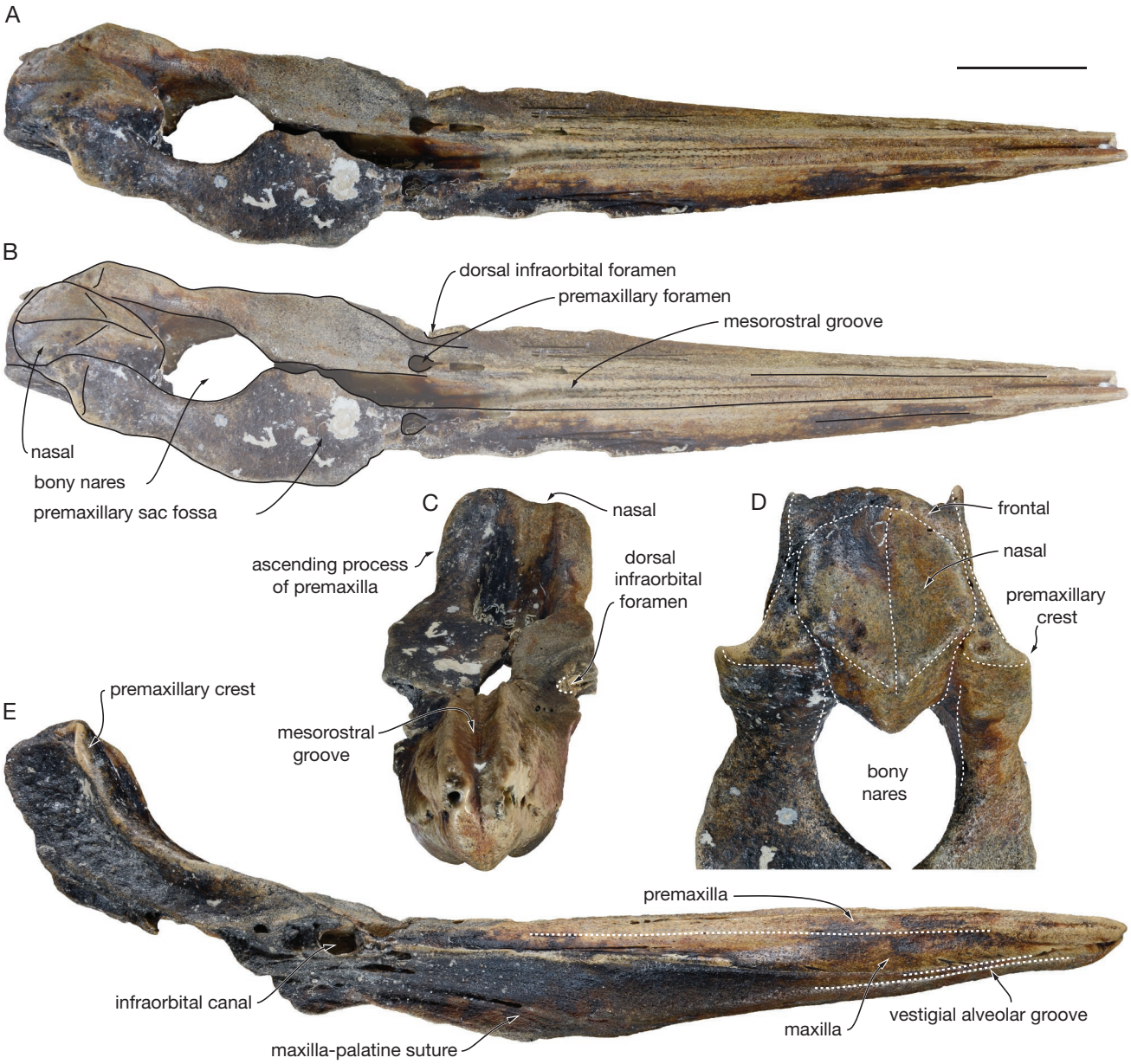

FIG. 13. — Partial cranium of *Nenga* sp. aff. *Nenga meganasalis* (MNHN.F.COI11): **A**, dorsal view; **B**, same view with interpretive line drawing; **C**, anterodorsal view; **D**, detail of the vertex in dorsal view; **E**, right lateral view. Scale bar: 100 mm.

views of the holotype in Bianucci *et al.* 2007: fig. 24), and the sulci along the vomer in the mesorostral groove. The main difference concerns the antorbital region; as in *Pterocetus benguelae*, the specimen MNHN.F.COI10 lacks a prominential notch, and its antorbital notch is more widely open and relatively deeper than in the holotype of *X. hendeysi*. Furthermore, the anteromedial slope of the nasals is somewhat more pronounced and the lateral margins of the nasals diverge slightly more anteriorly as compared to the holotype, two features in an intermediary state between the holotype and *P. benguelae*. However, the larger *P. benguelae* differs markedly in the more anterior position of the premaxillary foramen, the transversely broader antorbital region, and the lower rostral maxillary crest.

Genus *Nenga*
Bianucci, Lambert & Post, 2007

TYPE AND ONLY REFERRED SPECIES. — *Nenga meganasalis* Bianucci, Lambert & Post, 2007 by original designation.

Nenga sp. aff. *Nenga meganasalis*
Bianucci, Lambert & Post, 2007

REFERRED SPECIMEN AND LOCALITY. — Partial cranium MNHN.F.COI11 including rostrum, premaxillary sac fossae, and vertex (Fig. 13); geographic coordinates 49°40'42.0"S, 63°44'18.0"E (Skiff Bank, 365 km SWW to Kerguelen Islands); depth 1263 m (Fig. 1).

TABLE 10. — Measurements (in mm) on the partial crania of *Nenga* sp. aff. *Nenga meganasalis* (MNHN.F.COI11) and *Nenga meganasalis* (SAM PQ 69675 [holotype] and SAM PQ 2339 [from Bianucci *et al.* 2007]). Abbreviations: **+**, not complete; **–**, no data.

	Nenga* sp. aff. *Nenga meganasalis	***Nenga meganasalis***	
	MNHN.F.COI11	**SAM PQ 69675 (holotype)**	**SAM PQ 2339**
Distance between apex of rostrum and anteromedial angle of right bony naris	728	575	–
* Distance between apex of rostrum and posterior margin of left premaxillary foramen	609.5	482	–
Width of rostrum at half the length *	82	92	–
Height of rostrum at half the length *	77.5	80	–
Width of premaxillary sac fossae	159	156	147
Width of right premaxillary sac fossa	95	80	78
Width of left premaxillary sac fossa	60	64	58
Width of bony nares	66.5	69	66
Minimum width of right ascending process of premaxilla	35	38	–
Minimum width of left ascending process of premaxilla	25	–	–
Width of premaxillary crests	+131	+140	+133
Width of right premaxillary crest	+47.5	–	+35
Width of left premaxillary crest	+33	39	–
Minimum distance between premaxillary crests	50	69	64
Maximum width of nasals	65.5	92	93
Maximum width of right nasal	35	–	–
Maximum width of left nasal	30.5	–	–
Minimum distance between maxillae across vertex	57.5	93	102

BRIEF DESCRIPTION AND COMPARISON

Although missing the antorbital regions, this skull is characterized by an elongated rostrum, with a cross section at mid-length roughly as wide as high. On the anterior half of the rostrum the wavy floor of the alveolar groove suggests the presence of shallow, vestigial alveoli. Along its posterior half, the lateral margin of the rostrum diverges posterolaterally, as a relatively thin crest whose posterolateralmost portion is missing. The mesorostral groove is only partly filled with the vomer; the posteriormost part of the groove is empty, with the transversely concave floor rising anterodorsally. A large dorsal infraorbital foramen is partly preserved on the maxilla, at the same anteroposterior level as the premaxillary foramen. This foramen is followed anteriorly by a transversely concave area. The premaxillary foramen is relatively distant from the bony nares and close medially to the mesorostral groove. The premaxillary sac fossae are proportionally long, with a progressive posterodorsal rise. The right premaxillary sac fossa is much wider than the left, with a markedly rounded lateral margin in dorsal view. The dorsal surface is slightly transversely concave and the anteromedial angle is well defined. The narrow left fossa is similarly slightly transversely concave, with a less marked anteromedial angle. Taking into account that the lateralmost surface of the premaxillary crests is probably somewhat abraded, the lateral margin of each ascending process of the premaxilla is barely constricted in anterior view. The anterior surface of each premaxillary crest is not vertical. The left premaxillary crest is directed laterally, whereas the right is directed laterally and slightly posterolaterally. The nasals occupy a large part of the dorsal surface of the vertex, with a maximum width roughly at mid-length; they do not contribute to the corresponding premaxillary crest. The dorsal surface forms a shallow medial depression, without any marked anteroventral slope. The anteromedial tip of the joined nasals is slightly anterior to the premaxillary crests. The frontals are preserved on the vertex as a relatively short stripe of bone.

The large size of the nasals on the vertex, the transversely directed premaxillary crest, the lateral margin of the proportionally long ascending process of the premaxilla barely constricted in anterior view, and the long and highly asymmetric premaxillary sac fossae are features shared with *Nenga meganasalis*. In addition, the absence of filling of the posterior part of the mesorostral groove in MNHN.F.COI11 may indicate some degree of development of the presphenoid in this region, as seen in one specimen of *N. meganasalis* (SAM PQ 69676). Most of the measurements of COI11 correspond well with the cranial dimensions of *N. meganasalis*, except for the distinctly longer rostrum (as compared to the holotype of *N. meganasalis*, possibly lacking only a short part of the apex; Table 10) and the narrower nasals in the former. These differences and the fragmentary state of COI11 (see for example the poorly preserved dorsal surface of the rostrum) prevent from a firm attribution to the species *N. meganasalis*.

RADIOMETRIC DATING (^{14}C) FOR *MESOPLODON* SP. AFF. *M. LAYARDII*

The results of the analysis of the two samples are shown in Table 11. The values obtained indicate that the quality parameters of the collagen are excellent in both samples. The stable isotope ratios are consistent with the marine environment.

The calibrated results (including correction for the reservoir effect) are shown in Table 12, with all dates (BP, calBP and uncertainties) rounded to the nearest 5. The specimen

TABLE 11. — Results of the radiometric (^{14}C) dating of two specimens of *Mesoplodon* sp. aff. *M. layardii* (MNHN.F.COI5 and COI6), including uncalibrated dates and parameters of collagen quality assessment (see Material and methods section).

Specimen	Lab number	age BP	sigma	C%	N%	C/N ratio	δ13C (‰)	δ15N (‰)
MNHN.F.COI5	GrA 65316	9490	50	39.0	14.0	3.3	–16.5	13.6
MNHN.F.COI6	GrA 64025	11040	50	43.9	16.9	3.0	–15.7	12.1

MNHN.F.COI5 yields an age of 10 270-10 200 calBP (earliest Holocene) and the specimen COI6 an age of 12 670-12 575 calBP (latest Pleistocene). The calibrated date ranges are given at 1-sigma confidence level.

TABLE 12. — Calibrated ^{14}C dates for two specimens of *Mesoplodon* sp. aff. *M. layardii* MNHN.F.COI5 and COI6.

Specimen	Lab number	calBP (1sigma)	calBP (2sigma)
MNHN.F.COI5	GrA 65316	10270-10200	10395-10180
MNHN.F.COI6	GrA 64025	12670-12575	12715-12535

DISCUSSION AND CONCLUSIONS

Faunal comparison and geochronological age

Due to their discovery on the seafloor, apart from the radiometrically dated three specimens of *Mesoplodon* sp. aff. *M. layardii*, the geochronological age of the specimens studied here is currently unknown. The faunal comparison may still provide some clues. Indeed, at least four species (*Africanacetus ceratopsis*, *Izikoziphius rossi*, *Xhosacetus hendeysi*, and *Ziphius* sp.) of the Crozet-Kerguelen sample are shared with the South African assemblage, suggesting a roughly similar age for at least part of the fauna. Also originating from deep-sea deposits, the South African fossils were found associated to phosphorites. The last significant phosphogenesis episod for the South African western continental shelf being dated from the middle to early late Miocene (Compton *et al.* 2004; Wigley & Compton 2006), it is probable that at least part of the Crozet-Kerguelen assemblage dates from the Miocene. Such an assumption is further supported by the radiometric dating of the ferro-manganese crust surrounding a skull of *Africanacetus gracilis* found in deep-sea deposits off Brazil; $^{187}Os/^{188}Os$ ratio indicates a minimum age of 5 million years for this specimen (Ichishima *et al.* 2017; Nozaki *et al.* 2017). Pending similar analyses on Crozet-Kerguelen crania, a pre-Pliocene age can be reasonably proposed for at least part of the sample. In this context, it is worth noting that an important depositional hiatus is recorded from the late middle Miocene to the late Pliocene in two ODP sites (1139 and 1140) nearby some of the fossil crania discovered off Kerguelen Islands (Bénard *et al.* 2010). Such a hiatus may suggest that the ziphiid specimens originate from either middle Miocene or Pleistocene-Holocene levels. As demonstrated above, two specimens of *Mesoplodon* sp. aff. *Mesoplodon layardii* are dated from the latest Pleistocene and earliest Holocene, matching thus well the deposits above the hiatus. As discussed above, most other specimens described here are most likely considerably older, and may thus originate from middle Miocene levels. An alternative interpretation is that these ziphiid crania were buried in younger sediments (for example from the late Miocene), which were at some point reworked by deep-sea currents. However, in this case the upper part of the Miocene microfossil faunas would most likely have been composed of a mix of middle and late Miocene taxa, which is not the case in the two nearby ODP sites (Reusch 2002; Arney *et al.* 2003; McCartney *et al.* 2003). Another scenario similarly not invalidating a late Miocene age would imply the deposition of the crania during a time with locally reduced sedimentation, or even absence of sedimentation. Radiometric dating of several crania from the Crozet-Kerguelen assemblage and a more detailed analysis of the local geological/sedimentological context (for example investigating the presence/absence of phosphorite layers) will be necessary to choose between these interpretations and to better constrain the geochronological ages of the faunas considered here as well as the timing of the extinction of their members.

Palaeobiogeography and Palaeoecology

The record of at least four species from the South African assemblage in a region that is: 1) several thousands of kilometers distant from the southern tip of South Africa; and 2) farther south in the Southern Ocean increases considerably their paleobiogeographic range. Indeed, nowadays among ziphiid species occasionally or regularly observed off the southern coast of South Africa, not all appear to be distributed farther south (e.g. *Indopacetus pacificus* (Longman, 1926), *Mesoplodon densirostris*, and *M. mirus* True, 1913; Ross 1984; McLeod *et al.* 2006). New fossil records in the Crozet-Kerguelen area thus indicate a Southern Ocean distribution for *Africanacetus ceratopsis*, *Izikoziphius rossi*, *Xhosacetus hendeysi*, and *Ziphius* sp.

Interestingly, the Crozet-Kerguelen assemblage only includes members of the clade Hyperoodontinae + Ziphiinae (*sensu* Bianucci *et al.* 2016), and like the South African assemblage it lacks any stem ziphiid. Together, these two assemblages may suggest that stem ziphiids did not colonize the pelagic areas of the Southern Ocean, whereas their fossil remains are encountered in North Atlantic deep-sea deposits (Bianucci *et al.* 2013, 2016). Additional sampling from the Crozet-Kerguelen area and other Southern Ocean deep-sea localities will further test this hypothesis.

The size range occupied by the taxa found in the Crozet-Kerguelen area is similar to that of the South African fossil assemblage (see Bianucci *et al.* 2008), with species ranging

from small (body length estimates close to 4 m for *Khoikhoicetus kergueleni* n. sp.) to very large size (body length estimates beyond 8 m for *Ziphius* sp.). Nowadays, the smallest ziphiid species recorded in the Southern Ocean is probably *Mesoplodon grayi*, with a maximum body length not greater than 4.8 m, whereas the largest is *Berardius arnuxii*, culminating at more than 9 m (McLeod 2006). It is thus possible that the minimum body length of ziphiids from the Southern Ocean and neighbouring areas increased to some extent before reaching the present state.

A subset of the Crozet-Kerguelen assemblage deserves some more words of discussion. As mentioned above, ^{14}C dating of two specimens referred to *Mesoplodon* sp. aff. *Mesoplodon layardii* yielded latest Pleistocene-earliest Holocene ages. Most likely partly related to a preservation and collection bias, the number of cetacean taxa recorded from Pleistocene deposits worldwide is low (Uhen & Pyenson 2007). Such a trend is also recovered for Ziphiidae, with only a few ziphiid remains reported from the Pleistocene-early Holocene and, among those, an even smaller amount having been radiometrically dated (e.g. Aaris-Sørensen *et al.* 2010; Oishi & Hasegawa 1994; Paleobiology Database cetacean data compiled by M. D. Uhen). In this context the new records from the Crozet-Kerguelen assemblage are thus especially important. These cranial remains being relatively fragmentary, we can only suggest that they represent a new species, closely related to *M. layardii*. If confirmed (via DNA extraction or the discovery of more complete specimens), this hypothesis would indicate the presence of a currently unknown species of *Mesoplodon* in the Southern Ocean about 10 000 years ago. Either such a species went extinct in this short interval of time, or it may still exist today. Indeed, several new extant ziphiid species were recently described from different parts of the world (Reyes *et al.* 1991; Dalebout *et al.* 2002, 2014; Morin *et al.* 2017), and whales living in the Southern Ocean are less likely to be found stranded compared to less remote oceanic regions.

Acknowledgements
We would like to thank masters, crew, and fishery observers on board the French longliners operating in the Kerguelen and Crozet exclusive economic zones (EEZs); T. Clot and Direction des Pêches et des Questions Maritimes (DPQM) from Terres Australes et Antarctiques Françaises (TAAF) for their constant logistic efforts and financial support to transfer the heavy samples from Réunion island to MNHN (Paris); N. Gasco for discussions on longline fishing techniques; K. Post for advice on radiometric datings and for facilitating the transfer of samples to Groningen University; G. Bianucci for discussions on ziphiid paleontology and for providing the photos of *Khoikhoicetus agulhasis* and *Mesoplodon layardii*; M. D. Uhen for his effort compiling cetacean data in the Paleobiology Database; and P. Loubry for the excellent photographic work. Constructive comments from the two reviewers G. Bianucci and H. Ichishima considerably improved the quality of this work.

REFERENCES

Aaris-Sørensen K., Rasmussen K. L., Kinze C. & Petersen K. S. 2010. — Late Pleistocene and Holocene whale remains (Cetacea) from Denmark and adjacent countries: species, distribution, chronology, and trace element concentrations. *Marine Mammal Science* 26: 253-281. https://doi.org/10.1111/j.1748-7692.2009.00356.x

Aerts-Bijma A. T., van der Plicht J. & Meijer H. A. J. 2001. — Automatic AMS sample combustion and CO_2 collection. *Radiocarbon* 43: 293-298. https://doi.org/10.1017/S0033822200038133

Ambrose S. H. 1990. — Preparation and characterization of bone and tooth collagen for isotopic analysis. *Journal of Archaeological Science* 17: 431-451. https://doi.org/10.1016/0305-4403(90)90007-R

Arney J. E., McGonigal K. L., Ladner B. C. & Wise Jr S. W. 2003. — Lower Oligocene to middle Miocene diatom biostratigraphy of ODP site 1140, Kerguelen plateau, *in* Frey F. A., Coffin M. F., Wallace P. J. & Quilty P. G. (eds), *Proceedings ODP, Scientific Results* 183: 1-21. https://doi.org/10.2973/odp.proc.sr.183.009.2003

Bénard F., Callot J.-P., Vially R., Schmitz J., Roest W., Patriat M., Loubrieu B. & Team T. E. 2010. — The Kerguelen plateau: Records from a long-living/composite microcontinent. *Marine and Petroleum Geology* 27: 633-649. https://doi.org/10.1016/j.marpetgeo.2009.08.011

Bianucci G., Lambert O. & Post K. 2007. — A high diversity in fossil beaked whales (Odontoceti, Ziphiidae) recovered by trawling from the sea floor off South Africa. *Geodiversitas* 29: 5-62.

Bianucci G., Post K. & Lambert O. 2008. — Beaked whale mysteries revealed by sea floor fossils trawled off South Africa. *South African Journal of Science* 104 (3-4): 140-142. http://ref.scielo.org/8ygs3h

Bianucci G., Mijár I., Lambert O., Post K. & Mateus O. 2013. — Bizarre fossil beaked whales (Odontoceti, Ziphiidae) fished from the Atlantic Ocean floor off the Iberian Peninsula. *Geodiversitas* 35: 105-153. https://doi.org/10.5252/g2013n1a6

Bianucci G., Di Celma C., Urbina M. & Lambert O. 2016. — New beaked whales from the late Miocene of Peru and evidence for convergent evolution in stem and crown Ziphiidae (Cetacea, Odontoceti). *PeerJ* 4: e2479. https://doi.org/10.7717/peerj.2479

Buono M. R. & Cozzuol M. A. 2013. — A new beaked whale (Cetacea, Odontoceti) from the Late Miocene of Patagonia, Argentina. *Journal of Vertebrate Paleontology* 33: 986-997. https://doi.org/10.1080/02724634.2013.752377

Compton J. S., Wigley R. A. & McMillan I. K. 2004. — Late Cenozoic phosphogenesis on the western shelf of South Africa in the vicinity of the Cape Canyon. *Marine Geology* 206: 19-40. https://doi.org/10.1016/j.margeo.2004.02.004

Cottin J.-Y., Michon G. & Delpech G. 2011. — The Kerguelen volcanic Plateau: the second largest oceanic Igneous Province (LIP) on earth and a witness of the Indian Ocean opening, *in* Duhamel G. & Welsford D. (eds), *The Kerguelen Plateau: Marine Ecosystem and Fisheries*. Société française d'Ichthyologie, Paris: 29-42.

Dalebout M. L., Mead J. G., Baker C. S., Baker A. N. & van Helden A. L. 2002. — A new species of beaked whale *Mesoplodon perrini* sp. n. (Cetacea: Ziphiidae) discovered through phylogenetic analyses of mitochondrial DNA sequences. *Marine Mammal Science* 18: 577-608. https://doi.org/10.1111/j.1748-7692.2002.tb01061.x

Dalebout M. L., Baker C. S., Steel D., Thompson K., Robertson K. M., Chivers S. J., Perrin W. F., Goonatilake M., Anderson R. C., Mead J. G., Potter C. W., Thompson L., Jupiter D. & Yamada T. K. 2014. — Resurrection of *Mesoplodon hotaula* Deraniyagala 1963: A new species of beaked whale in the tropical Indo-Pacific. *Marine Mammal Science* 30: 1081-1108. https://doi.org/10.1111/mms.12113

DeNiro M. J. 1985. — Postmortem preservation and alteration of in vivo bone collagen isotope ratios in relation to paleodietary reconstruction. *Nature* 317: 806-809. https://doi.org/10.1038/317806a0

Duhamel G. & Williams R. 2011. — History of whaling, sealing, fishery and aquaculture trials in the area of the Kerguelen Plateau, *in* Duhamel G. & Welsford D. (eds), *The Kerguelen Plateau: Marine Ecosystem and Fisheries*. Société française d'Ichthyologie, Paris: 15-28.

Gol'din P. E. & Vishnyakova K. A. 2012. — *Africanacetus* from the sub-Antarctic region: the southernmost record of fossil beaked whales. *Acta Palaeontologica Polonica* 58: 445-452. https://doi.org/10.4202/app.2011.0097

Hale H. M. 1931. — Beaked whales, *Hyperoodon planifrons* and *Mesoplodon layardii*, from South Australia. *Records of the South Australian Museum* 4: 291-311. https://biodiversitylibrary.org/page/41026494

Heyning J. E. 1989. — Comparative facial anatomy of beaked whales (Ziphiidae) and a systematic revision among the families of extant Odontoceti. *Contributions in Science, Natural History Museum of Los Angeles County* 405: 1-64.

Heyning J. E. & Mead J. G. 1996. — Suction feeding in beaked whales: morphological and observational evidence. *Contributions in Science, Natural History Museum of Los Angeles County* 464: 1-12.

Ichishima H., Augustin A. H., Toyofuku T. & Kitazato H. 2017. — A new species of *Africanacetus* (Odontoceti: Ziphiidae) found on the deep ocean floor off the coast of Brazil. *Deep Sea Research Part II*. https://doi.org/10.1016/j.dsr2.2016.12.002

Lambert O., Buffrénil V. de & Muizon C. de 2011. — Rostral densification in beaked whales: diverse processes for a similar pattern. *Comptes Rendus Palevol* 10: 453-468. https://doi.org/10.1016/j.crpv.2011.03.012

Longin R. 1971. — New method of collagen extraction for radiocarbon dating. *Nature* 230: 241-242. https://doi.org/10.1038/230241a0

McCartney K., Engel R., Reed T., Williamson R., Bohaty S. M. & Wise Jr, S. W. 2003. — Silicoflagellates from ODP Holes 1138A and 1140A, Kerguelen Plateau, *in* Frey F. A., Coffin M. F., Wallace P. J. & Quilty P. G. (eds), *Proceedings ODP, Scientific Results* 183: 1-20.

McLeod C. D. 2006. — How big is a beaked whale? A review of body length and sexual size dimorphism in the family Ziphiidae. *Journal of Cetacean Research and Management* 7: 301-308.

McLeod C. D., Santos M. B. & Pierce G. J. 2003. — Review of data on diets of beaked whales: Evidence of niche separation and geographic segregation between three genera. *Journal of the Marine Biological Association of the United Kingdom* 83: 651-655. https://doi.org/10.1017/S0025315403007616h

McLeod C. D., Perrin W. F., Pitman R., Barlow J., Ballance L., D'Amico A., Gerrodette T., Joyce G., Mullin K. D., Palka D. L. & Waring G. T. 2006. — Known and inferred distributions of beaked whale species (Cetacea: Ziphiidae). *Journal of Cetacean Research and Management* 7: 271-286.

Mead J. G. 1989a. — Beaked whales of the genus *Mesoplodon*, *in* Ridgway S. H. & Harrison R. (eds), *Handbook of Marine Mammals, Vol. 4: River Dolphins and the Larger Toothed Whales.* Academic Press, London: 349-430.

Mead J. G. 1989b. — Bottlenose whales *Hyperoodon ampullatus* (Forster, 1770) and *Hyperoodon planifrons* Flower, 1882, *in* Ridgway S. H. & Harrison R. (eds), *Handbook of Marine Mammals, Vol. 4: River Dolphins and the Larger Toothed Whales.* Academic Press, London: 321-348.

Mead J. G. & Fordyce R. E. 2009. — The therian skull: a lexicon with emphasis on the odontocetes. *Smithsonian Contributions to Zoology* 627: 1-248. https://doi.org/10.5479/si.00810282.627

Mook W. G. 2006. — *Introduction to Isotope Hydrology: Stable and Radioactive Isotopes of Hydrogen, Oxygen and Carbon*. Taylor and Francis, London, 256 p.

Mook W. G. & Streurman H. J. 1983. — Physical and chemical aspects of radiocarbon dating. *PACT Publications* 8: 31-55.

Mook W. G. & van der Plicht J. 1999. — Reporting ^{14}C activities and concentrations. *Radiocarbon* 41: 227-239. https://doi.org/10.1017/S0033822200057106

Morin P. A., Scott Baker C., Brewer R. S., Burdin A. M., Dalebout M. L., Dines J. P., Fedutin I., Filatova O., Hoyt E. & Jung J. L. 2017. — Genetic structure of the beaked whale genus *Berardius* in the North Pacific, with genetic evidence for a new species. *Marine Mammal Science* 33: 96-111. https://doi.org/10.1111/mms.12345

Nozaki T., Takaya Y., Toyofuku T., Tokumaru A., Goto K. T., Chang Q., Kimura J.-I., Kato Y., Suzuki K. & Augustin A. H. 2017. — Depositional age of a fossil whale bone from São Paulo Ridge, South Atlantic Ocean, based on Os isotope stratigraphy of a ferromanganese crust. *Resource Geology* 67: 442-450.

Oishi M. & Hasegawa Y. 1994. — A list of fossil cetaceans in Japan. *The Island Arc* 3: 493-505. https://doi.org/10.1111/j.1440-1738.1994.tb00128.x

Ramassamy B. 2016. — Description of a new long-snouted beaked whale from the Late Miocene of Denmark: evolution of suction feeding and sexual dimorphism in the Ziphiidae (Cetacea: Odontoceti). *Zoological Journal of the Linnean Society* 178: 381-409. https://doi.org/10.1111/zoj.12418

Reimer P. J., Bard E., Bayliss A., Beck J. W., Blackwell P. G., Bronk Ramsey C., Buck C. E., Edwards R. L., Friedrich M., Grootes P. M., Guilderson T. P., Haflidason H., Hajdas I., Hatté C., Heaton T. J., Hoffmann D. L., Hogg A. G., Hughen K. A., Kaiser K. F., Kromer B., Manning S. W., Niu M., Reimer R. W., Richards D. A., Scott E. M., Southon J. R., Staff R. A., Turney C. S. M. & van der Plicht J. 2013. — IntCal13 and Marine13 Radiocarbon age calibration curves 0-50,000 years cal BP. *Radiocarbon* 55: 1869-1887. https://doi.org/10.2458/azu_js_rc.55.16947

Reusch D. N. 2002. — Oligocene–Miocene terrigenous and pelagic sediments, Skiff Bank, Kerguelen Plateau (ODP Leg 183, Site 1139), *in* Frey F. A., Coffin M. F., Wallace P. J. & Quilty P. G. (eds), *Proceedings ODP, Scientific Results* 183: 1-31.

Reyes J. C., Mead J. G. & Van Waerebeek K. 1991. — A new species of beaked whale *Mesoplodon peruvianus* sp. n. (Cetacea: Ziphiidae) from Peru. *Marine Mammal Science* 7: 1-24. https://doi.org/10.1111/j.1748-7692.1991.tb00546.x

Robineau D. 1973. — Sur deux rostres de *Mesoplodon* (Cetacea, Hyperoodontinae). *Mammalia* 37: 504-513.

Ross G. J. B. 1984. — The smaller cetaceans of the south east coast of southern Africa. *Annals of the Cape Provincial Museums of Natural History* 15: 173-410.

Schorr G. S., Falcone E. A., Moretti D. J. & Andrews R. D. 2014. — First long-term behavioral records from Cuvier's beaked whales (*Ziphius cavirostris*) reveal record-breaking dives. *PLoS ONE* 9: e92633. https://doi.org/10.1371/journal.pone.0092633

True F. W. 1910. — An account of the beaked whales of the family Ziphiidae in the collection of the United States National Museum, with remarks on some specimens in other American museums. *Bulletin of the United States National Museum* 73: 1-89.

Turner W. 1880. — Report on the bones of Cetacea collected during the voyage of HMS Challenger in the years 1873-1876, *in* Thomson C. W. (ed.), *Report on the Scientific Results of the Voyage of HMS Challenger, Zoology, Vol. 1*. Neill and Company, Edinburgh: 1-45.

Tyack P. L., Johnson M., Aguilar de Soto N., Sturlese A. & Madsen P. T. 2006. — Extreme diving of beaked whales. *Journal of Experimental Biology* 209: 4238-4253. https://doi.org/10.1242/jeb.02505

UHEN M. D. & PYENSON N. D. 2007. — Diversity estimates, biases, and historiographic effects: resolving cetacean diversity in the Tertiary. *Palaeontologia Electronica* 10: 1-22.

VAN BENEDEN P.-J. & GERVAIS P. 1880. — *Ostéographie des cétacés vivants et fossiles*. Arthus Bertrand, Paris, 634 p. https://doi.org/10.5962/bhl.title.50302

VAN DER PLICHT J., WIJMA S., AERTS A. T., PERTUISOT M. H. & MEIJER H. A. J. 2000. — The Groningen AMS facility: status report. *Nuclear Instruments and Methods* B172: 58-65. https://doi.org/10.1016/S0168-583X(00)00284-6

WIGLEY R. A. & COMPTON J. S. 2006. — Late Cenozoic evolution of the outer continental shelf at the head of the Cape Canyon, South Africa. *Marine Geology* 226: 1-23. https://doi.org/10.1016/j.margeo.2005.09.015

Submitted on 7 September 2017;
accepted on 24 November 2017;
published on 29 March 2018.